THESIS

INVESTIGATING THE CARBONATE-SHALE FACIES TRANSITION AND DEPOSITION ON THE SCANDINAVIAN ORDOVICIAN SHELF – THE ARNESTAD FORMATION, SOUTHERN NORWAY

Submitted by

Kathryn M. Schuller

Department of Geosciences

In partial fulfillment of the requirements

For the Degree of Master of Science

Colorado State University

Fort Collins, Colorado

Spring 2018

Master's Committee:

Advisor: Sven O. Egenhoff

Dario Harazim
Derek Schutt
Joe von Fischer

ABSTRACT

INVESTIGATING THE CARBONATE-SHALE FACIES TRANSITION AND DEPOSITION ON THE SCANDINAVIAN ORDOVICIAN SHELF – THE ARNESTAD FORMATION, SOUTHERN NORWAY

The Upper Ordovician Arnestad Formation was located on the northwestern edge of Baltica in the region near modern day Oslo, Norway. This formation was found to be 60 m thick and consists of intercalated siliciclastic mudstones and thin, nodular carbonate beds. Six outcrops and 38 thin sections were used to describe the Arnestad Formation in detail and divide the formation into six key facies. Dark grey silicilastic mudstones dominate the succession and contain lenses of fossil fragments. Interbedded nodular carbonates are mud- to wackestones, contain lenses of fossil fragments, and often form continuous beds. All facies show varying amounts of bioturbation from *Chondrites,* and *Phycosiphon*-like fecal strings can be found in the siliciclastic mudstone facies. The Arnestad Formation can be divided stratigraphically into a lower portion with siliciclastic mudstones and continuous carbonate beds, a central part dominated by siliciclastic mudstones with local ash and carbonate beds, and an upper portion containing both thick siliciclastic mudstone beds and intercalated stacks of siliciclastic and carbonate mudstones.

The Arnestad Formation is interpreted as representing sedimentation on a ramp-like shelf with carbonate facies deposited proximally to siliciclastic mudstone facies, below normal wave base with sediment and bioclasts being transported basinward due to bed load processes. Fair-weather and storm generated deposits are found in all facies, with storms eroding the sediment

and producing shell lenses throughout the formation, but increasing in frequency upwards independent of sea-level. In the lower part of the succession, the Arnestad Formation records a relatively low sea-level stand, shifting to an overall high sea-level position during the middle part, and back to another low sea-level position in the upper portion. Ash beds are found almost exclusively in the middle portion and seem to have higher preservation potential during high versus low sea-level positions. There were likely more ash beds deposited than were found that were later biogenitically homogenized, rendering the beds mostly unrecognizable from the surrounding sediment. The frequent intercalation of the siliciclastic mudstones with carbonate beds most likely shows the influence of climate cycles on deposition. Based on dividing the length of deposition (~3.5 my) by the estimated cycle count (215 – 220), these small-scale cycles were found to have periods between 15,900 and 16,300 years and are interpreted as precessional Milankovitch cycles.

ACKNOWLEDGMENTS

I would like to thank AAPG for providing funding to carry out the research for this project. I am also grateful to my advisor, Dr. Sven Egenhoff, for his patience and the all his efforts in reviewing, revising, and discussing this thesis. I am additionally appreciative to my thesis committee members: Dr. Sven Egenhoff, Dr. Dario Harazim, Dr. Derek Schutt, and Dr. Joe von Fischer. Their insightful suggestions helped improve the quality of this thesis, and their feedback and incisive comments greatly heightened my understanding of this study and of the related subject matter.

I want to give a very special thank you to all the members of the Colorado State University Sedimentology working group that I've had the pleasure to work with over the years. I am extremely appreciative of Heather Judd, Caroline Martin, and Kajal Nair for being there for all of the discussions, frustrations, and realizations that accompany the trials of completing a thesis. All the laughs, tears, and friendship mean more than words can describe. Most of all, I am beholden to my husband, Steve Nunn, for enduring throughout this process. He has been an immense source of encouragement, support, and love, and I could not have done it without him.

TABLE OF CONTENTS

1.0 INTRODUCTION

Siliciclastic mudstones that have been deposited in the distal reaches of carbonate ramp systems still present a challenge when trying to describe and fully understand their sedimentary environment and the processes that control their formation. Even though progress is being made in showing evidence of bedload transport processes in siliciclastic mudstones (e.g. Schieber 1998; Schieber et al., 2007; Macquaker et al., 2007), and describing mud distribution and transport in epicontinental basins (Schieber, 2016), many of these papers do not explicitly focus on the critical transition from carbonate to siliciclastic depositional environments. Also, carbonate ramp models generally exclude siliciclastic mudstones and focus solely on the carbonate facies (e.g. Ahr, 1973; Aigner, 1984; Colmbié et al., 2014; Amel, 2015). Moreover, the siliciclastic mudstones in carbonate ramp systems are generally relegated to only being deposited far into the basin in a low-energy environment through suspension settling processes under anoxic conditions (Burchette and Wright, 1992; Algeo et al., 2016). Nevertheless, recent examples suggest that many, if not most, mudstones were deposited under dysoxic conditions (Schieber and Yawar, 2009; Macquaker et al., 2010; Borcovsky et al., 2017), and the once believed homogenous siliciclastic mudstone environment can be subdivided into several distinctly different facies belts (e.g. Egenhoff et al., 2015; Borcovsky et al., 2017). In these studies, proximal siliciclastic mudstones only occupy a small portion of the succession. Moreover, formations consisting entirely of proximal mudstones are unknown to date, especially because most studies do not examine this transitional area between carbonates and siliciclastic mudstones. As such, it would be intriguing to explore the processes that lead to the formation of such thick proximal mudstone successions, and to emphasize which processes govern the fine-grained facies belts adjacent to the most distal carbonate realm.

The Arnestad Formation consists dominantly of siliciclastic mudstones interpreted to represent a proximal shale environment in this study. Nevertheless, a significant percentage of the succession is made up of depositional carbonates. This unit therefore reflects the recurrent alternation between a proximal siliciclastic mudstone facies located adjacent to carbonates, and a distal carbonate environment that in its far reaches borders siliciclastic mudstones. These repeated lithofacies changes document this crucial facies transition in great detail, yet they also permit an estimation of the driver behind these reoccurring sea-level changes.

This study is centered around the Ordovician Arnestad Formation, which is a highly cyclic, carbonate and siliciclastic mudstone system, deposited on a ramp-like carbonate shelf. The purpose of this study was twofold: 1) to more fully explore the depositional environment and unique stratigraphy of the Arnestad Formation, as it exposes sedimentation of siliciclastic mudstones in close proximity to a carbonate ramp depositional system; and 2) to describe and understand the frequency of the cycles in this unit, and a potential influence of climate forcing on this deep shelf succession. These results were based on detailed stratigraphic sections and facies analysis using 6 outcrops located near Oslo, Norway (Figure 1.1) and 38 thin sections from key sedimentological and stratigraphic intervals.

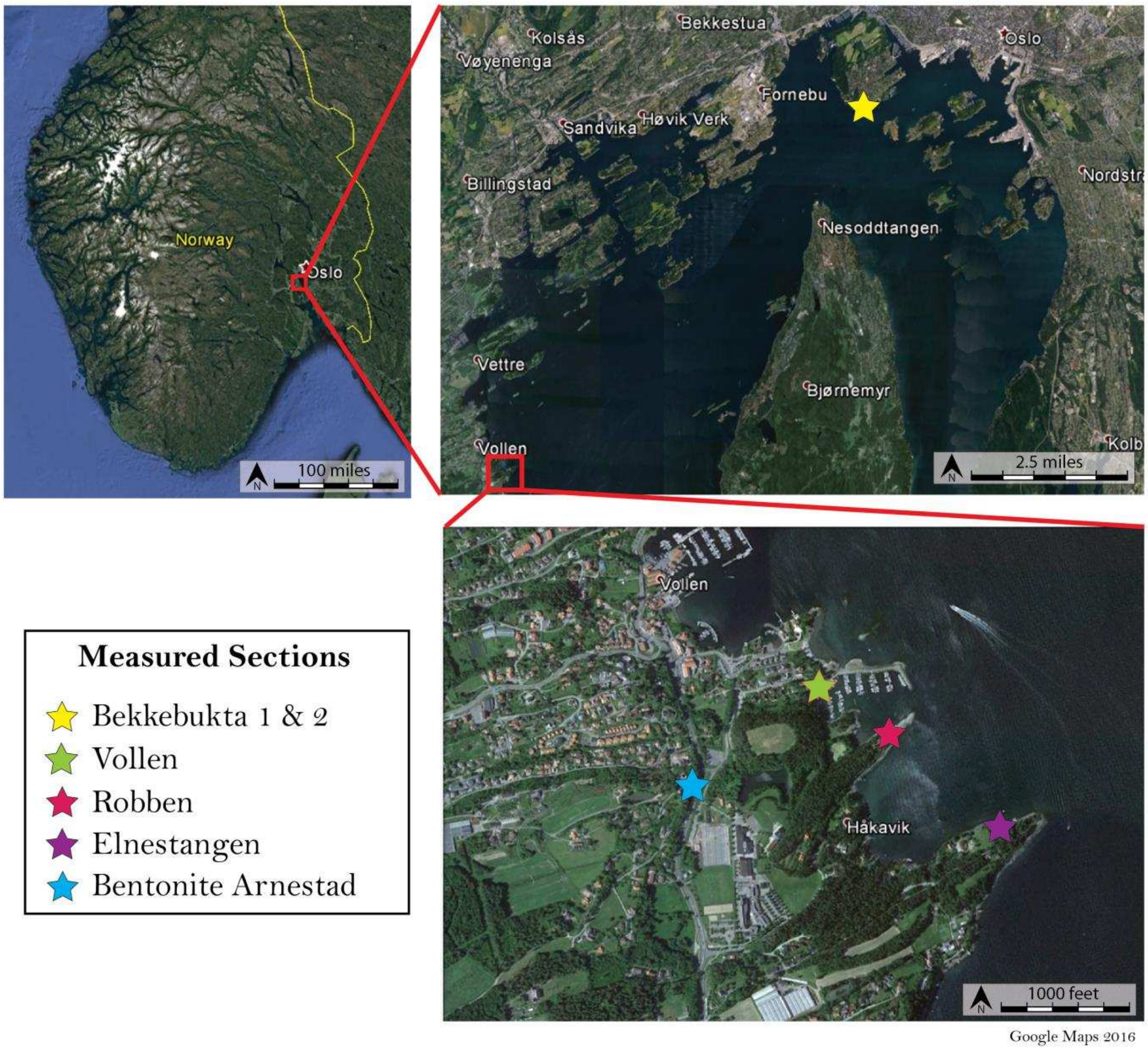

Figure 1.1: Map showing location of the study area near Oslo, Norway. Stars denote sections of the Arnestad Formation that were logged and sampled.

2.0 GEOLOGIC SETTING

During the Lower Ordovician, the Baltica terrane was located at fairly high latitudes between 40°S and 60°S (Cocks and Torsvik, 2005). Throughout the Ordovician, Baltica travelled northward, opening the Ran Ocean to the south and the Iapetus Ocean to the west of Baltica (Cocks and Torsvik, 2005). During this northward migration, Baltica experienced a ~120° counterclockwise rotation (Cocks and Torsvik, 2005), with Scandinavia located in its northeastern part during the Lower Ordovician and moving to its northwestern edge by the Early Silurian. The northward movement of Baltica started slowing down in the Upper Ordovician, and the terrane was located in lower latitudes near the paleoequator (Figure 2.1) during this time (Cocks and Torsvik, 2005).

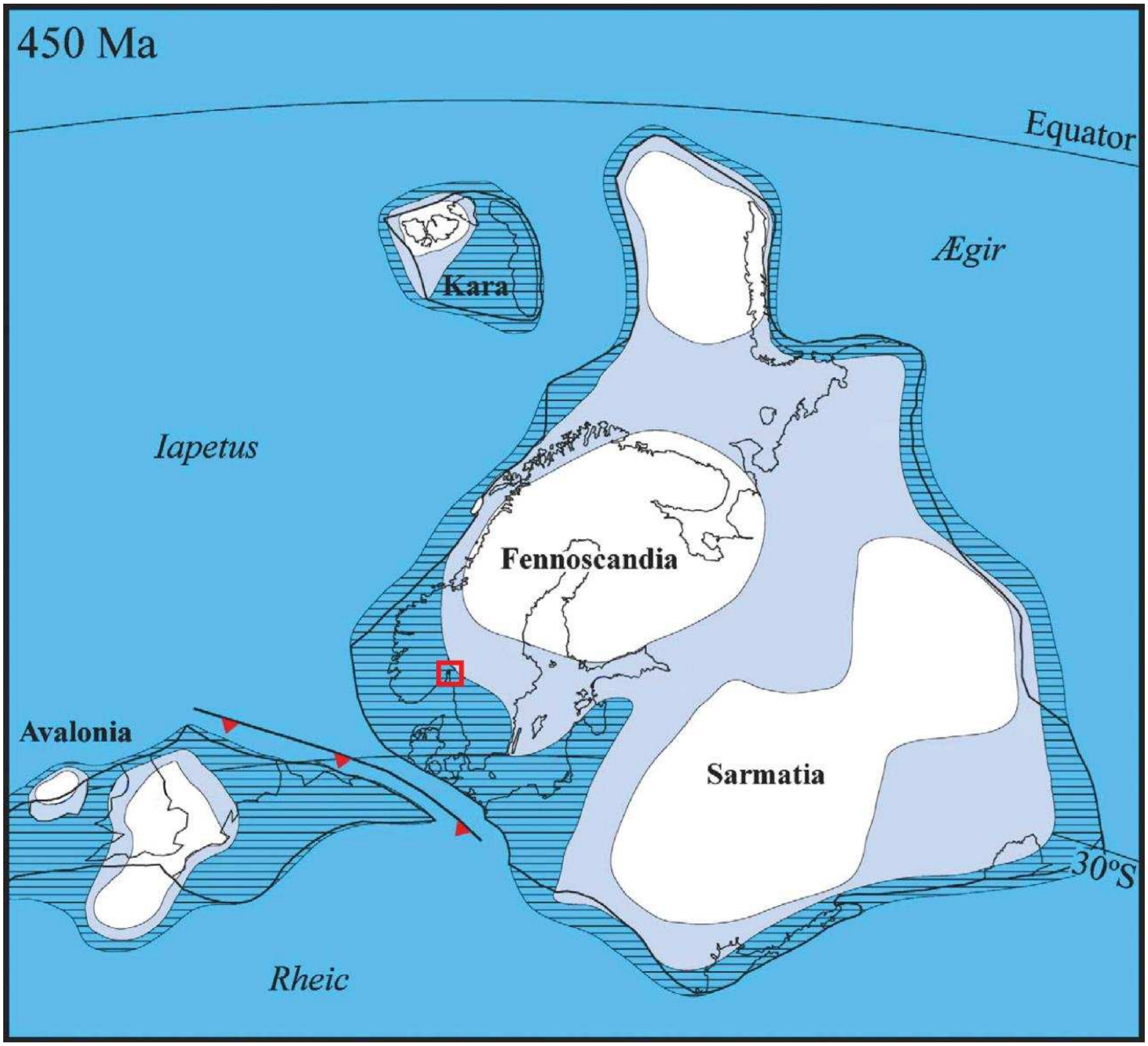

Figure 2.1: Paleogeography of Baltica terrane during the Late Ordovician, with the study area outlined in the red box. Land, shallow shelf, deeper shelf, and oceans are all represented. Modified from Cocks and Torsvik (2005).

Multiple island arcs characterized Baltica outboard of its northwestern margin during the Middle Ordovician. The volcanoes associated with the island arcs produced a multitude of bentonite beds (Bruton et al., 1985) that are widely distributed in Baltica as well as in the eastern part of Laurentia. The thickest of these ash layers is the Kinnekulle bentonite that measures up to 2 m in thickness in present-day southern Sweden (Bergström et al., 1995). As the Iapetus Ocean closed, the island arcs were successively accreted onto the Baltica terrane (Cocks and Torsvik, 2005).

During the Ordovician, the climate was influenced by extended greenhouse conditions (Munnecke et al., 2010). Climate curves constructed from isotope data, in conjunction with sea-level curves (Nielsen, 2004,) show generally warm conditions followed by a notable icehouse interval at the Ordovician – Silurian boundary, known as Hirnantian glaciation. Warm oceanic waters during this time increased the diversity in benthic fauna in Scandinavia (Hansen and Harper, 2008), which is widely known worldwide as the Great Ordovician Biodiversification Event. Sedimentation also changed from primarily clastic with a few cold-water carbonates in the Cambrian and Lower Ordovician to warm-water carbonates and tropical reefs by the end of the Ordovician (Størmer, 1953; Bjørlykke, 1974a). However, there is growing evidence that there was cooling throughout the Early Ordovicain from Greenhouse (~42°C) to modern equatorial (~28°C) temperatures, and the climate stabilized at these lower temperatures during the mid- to late- Ordovician (Trotter et al., 2008).

The western margin of Baltica was the edge of a foreland basin (Greiling and Garfunkel, 2007), oriented NE-SW, formed during the Early Ordovician. However, due to the low relief of Baltica (Bjørlykke, 1974b) that was covered by an inland sea, sedimentation rates were fairly low (Bruton et al., 1985) and the basin filled with no more than 500 m of sediment (Greiling and Garfunkel, 2007). The sediment filling the basin was transported from the northwest (Greiling and Garfunkel, 2007), and as Baltica was migrating north and approaching the island arc chains in the northwest, it greatly influenced the composition of the sediment. With the increase in supply from the island arcs, there was an increase in chlorite, Fe, Mg, Ni, and Cr in the sediment deposited from Lower Ordovician to Upper Ordovician (Bjørlykke, 1974b).

In the Oslo region, the Lower Palaeozoic succession is generally well exposed and broadly consists of a basal black shale with small amounts of clastic sandstones in the Cambrian. Throughout the Ordovician, the geologic units transition to a succession of shales alternating with nodular to bedded limestones, and is capped by coral facies in the Silurian (Størmer, 1953; Bjørlykke, 1974a). Though the geologic units were originally described by Størmer in 1953, the Oslo-Asker region was more formally delineated and defined by Owen et al. in 1990.

In the Oslo-Asker region, the locally outcropping Arnestad Formation is around 40m thick and is Middle Ordovician (Caradoc) in age (Owen et al., 1990). It is bounded at its base by the Vollen Formation, which is predominantly composed of limestone that is recurrently interbedded with minor shales (Størmer, 1953; Owen et al. 1990) with infrequent fossils. The Arnestad Formation is overlain by the Frognerkilen Formation, which consists of closely packed limestone nodules that are rarely interbedded with thin shales (Størmer, 1953) and contains sparse fossils (Owen et al., 1990).

The Arnestad Formation was previously known as the 'Lower Chasmops Shale' or '4bα' and was described by Størmer (1953) as a black shale, with the lower part containing limestone nodules and the upper part having a few continuous limestone beds with some bentonite layers. Owen et al. (1990) more fully described the Arnestad Formation as having a basal section of thick dark shales with minor limestone beds, and several well-developed bentonites in the section, along with a substantial increase in the diversity of benthic shelly fossils in the formation (Owen et al., 1990) as compared to underlying units.

3.0 METHODOLOGY

This study encompasses data from both outcrop and petrographic descriptions from thin sections. Six different outcrops were studied in the Oslo-Asker region in Norway, by taking measured sections and samples from each location. The stratigraphic sections totaled 93.55m, and were measured at the cm-scale using a tape measure, and detailed notes were taken throughout the sections, which were later digitized using Adobe Illustrator CS5.1.

A total of thirty-five oriented rock samples were collected, with representative samples of the formation from each location, and making sure to include a wide range of both carbonates and mudstones. The mudstone samples were epoxied to keep the integrity of the samples intact, with thin sections created from all samples. All thin sections were prepared by TPS Enterprises, and were polished; the mudstones were made to a thickness of 20µm and the carbonates were 40µm thick. Thin section samples were then examined using Nikon Eclipse Ci-E, where composition, matrix, biogenic material, bioturbation index (Table 3.1), and other characteristics were described.

The matrix of four thin sections was analyzed using a scanning electron microscope (SEM) at the United States Geological Survey in Denver, Colorado. These thin sections were carbon-coated and examined using a Quatra 450 FEG scanning electron microscope equipped with an energy-dispersive X-Ray spectroscope (EDS) that includes a backscattered electron (BSE) Detector.

Table 3.1: Bioturbation Index (BI) as described by Taylor and Goldring, (1993).

Grade	Percent Bioturbated	Classification
0	0	No bioturbation
1	1 – 4	Sparse bioturbation, bedding distinct, few discrete traces and/or escape structures
2	5 – 30	Low bioturbation, bedding distinct, low trace density, escape structures often common
3	31 – 60	Moderate bioturbation, bedding boundaries sharp, traces discrete, overlap rare
4	61 – 90	High bioturbation, bedding boundaries indistinct, high trace density with overlap common
5	91 – 99	Intense bioturbation, bedding completely disturbed (just visible), limited reworking, later burrows discrete
6	100	Complete bioturbation, sediment reworking due to repeated overprinting

4.0 SEDIMENTOLOGY

The Arnestad Formation predominantly consists of siliciclastic mudstones interbedded with nodular carbonate beds, which are in the present study are subdivided into six facies and described below (Table 4.1), as well as one bentonite facies. Much of the Arnestad Formation is characterized by a limited amount of grain types and sedimentary structures, making any differentiation between facies a subtle distinction, though still recognizable.

Table 4.1: Summary of sedimentologic attributes of the facies in the Arnestad Formation. Bioturbation index (BI) is from Taylor and Goldring (1993).

Facies	Composition	Description and Sedimentary Structures	Interpretation
Facies 1: Fine siliciclastic mudstone	• Matrix: carbonate-rich • BI: 4 – 5; *Chondrites, Phycosiphon*-like fecal strings • Bioclasts: 1 – 5%; up to 0.5 mm in lenght; fragmented • Trilobites, brachiopods, echinoderms	• No observable sedimentary structures	• Abundant benthic life, obliterating any sedimentary structures • Well-abraded, small, fragmented bioclasts suggest bed load transport processes
Facies 2: Bioturbated siliciclastic mudstone with bioclasts	• Matrix: carbonate-rich; sub-angular, silt-size quartz grains (5 – 10%) • BI: 3 – 4; *Chondrites, Phycosiphon*-like fecal strings • Bioclasts: 5%; 0.5 – 1 mm long, rarely up to 8 mm; whole or fragmented • Trilobites, brachiopods, bryozoans, echinoderms, gastropods	• Rare sub-mm scale discontinuous parallel to curved horizontal laminae	• Abundant benthic life, obliterating most sedimentary structures • Sub-mm laminae seem to be superficial and the grains aligned as organisms burrowed through the sediment • Quartz and bioclast fragments brought in by bed load transport processes
Facies 3: Bioturbated carbonate mudstone	• Matrix: micrite • BI: 3 – 4; *Chondrites* • Bioclasts: 3 – 8%; 0.5 – 3 mm long; fragmented • Trilobites, brachiopods, bryozoans, echinoderms	• No observable sedimentary structures	• Moderate burrowing indicating a low energy, sub-tidal environment • Bioclasts were transported by bed load processes

Facies 4: Bioturbated carbonate wackestone	• Matrix: micrite • BI: 4 – 5; *Chondrites* • Bioclasts: 10 – 20%; 0.5 – 10 mm long; fragmented and whole • Trilobites, brachiopods, bryozoans, gastropods, echinoderms	• Rare sub-mm wavy horizontal laminae of dark brown silt-sized grains	• Abundant benthic life suggesting a low energy, sub-tidal environment • Bed load transport processes likely brought in smaller, fragmented bioclasts and the silt-sized grains, forming laminae as energy waned • Whole, large bioclasts indicate some organisms were autochthonous
Facies 5: Bioclastic packstone	• Matrix: micrite or siliciclastic mudstone; silt-sized, rounded carbonate grains • Bioclasts: up to 70%; generally 1 – 5 mm long, range from <1 mm up to 11 mm long; fragmented and whole • Trilobites, brachiobods, bryozoans, gastropods, echinoderms	• Form lenses generally 2 – 5 cm, up to 10 cm long • Bioclasts are randomly oriented and poorly sorted	• Large, broken bioclasts reflect a high-energy depositional environment transporting and fragmenting bioclasts • Poorly sorted and randomly oriented bioclasts in lenses suggests storm deposits or other high-energy events • Silt-sized, rounded carbonate grains indicate longer transport distances for some grains, while the larger, less fragmented or whole bioclasts show some shorter transport distances • Matrix composition was influenced by the surrounding sediment that settled in between the bioclasts as flow waned

Facies 6: Bioturbated bentonite	• Blue-green bentonite • Contains angular plagioclase and quartz grains; rounded carbonate grains • BI: 3; *Chondrites* • Burrows filled with a siliciclastic mud matrix, similar to facies 1	• Irregular wavy horizontal laminae	• Low energy environment allowing burrowing to occur, though some burrows were later filled with siliciclastic muds • Burrows disturbed the ash after deposition, giving it a wavy appearance

4.1 Facies 1 – Fine siliciclastic mudstone

Facies 1 is a dark grey to dark brown fine siliciclastic mudstone with a carbonate-rich matrix and also contains clay-size quartz, albite, illite, chlorite, as well as minor rutile. It contains discontinuous parallel horizontal laminae that are often faint and overprinted by burrows. The bioturbation index is 4 – 5 (Taylor & Goldring, 1993), and includes mostly *Chondrites* burrows, along with *Phycosiphon*-like fecal strings throughout this facies (Figure 4.1A). Burrow cross-sections tend to be horizontal and elongate, with a more clay-rich and organic-rich interior, with rare clusters of pyrite crystals, and silt along the margins of the burrows. This facies contains rare broken bioclasts (1 - 5%), which include trilobites, brachiopods, and echinoderms. Bioclast fragments are rounded, generally less than 0.5mm in length, and are scattered randomly throughout the facies. They are partially to fully recrystallized, though some fragments are preferentially replaced with pyrite (Figure 4.1B).

Facies 1 is intensely bioturbated which obliterated most primary sedimentary structures. Multiple types of organisms produced these burrows, indicated by the numerous *Chondrites* and *Phycosiphons* traces, reflecting abundant benthic life during deposition. These observations suggest that seafloor conditions were most likely dysoxic to oxic, and represent somewhat hospitable living conditions.

The fragmented nature of all bioclasts indicate that they must have been broken after the demise of the organism and prior to deposition. In addition, the rounded appearance of the bioclast fragments reveal abrasion, probably during transport of the particles, and indicate bed load transport during sedimentation. The organisms could have lived either in the Arnestad Formation shale environment or may have been transported to the place of sedimentation from an adjacent carbonate setting. Nevertheless, the scarcity of carbonate particles in this facies makes it likely that these organisms were allochthonous to this facies rather than autochthonous.

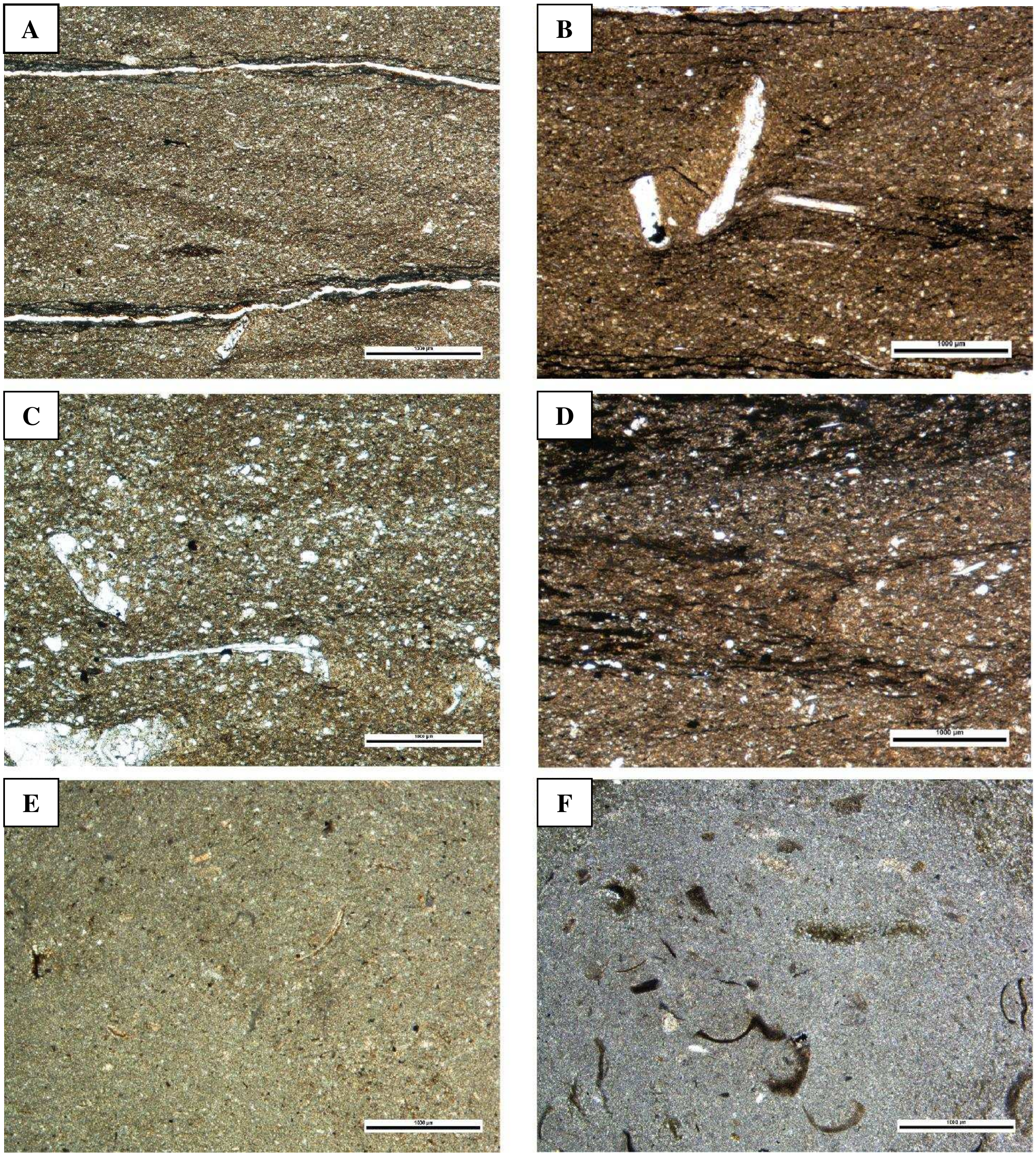

Figure 4.1: Thin section photos of the siliciclastic mudstone and carbonate facies of the Arnestad Formation; scale bar is 1 mm in all photos; **A)** fine siliciclastic mudstone (facies 1) with a carbonate-rich matrix and *Chondrites* burrows; **B)** fine siliciclastic mudstone (facies 1) with recrystallized bioclasts, including pyrite replacement; **C)** bioturbated siliciclastic mudstone with bioclasts (facies 2) showing bioclasts and sub-angular, silt-size quartz grains; **D)** bioturbated siliciclastic mudstone with bioclasts (facies 2) showing *Chondrites* burrow outlined in sub-mm discontinuous horizontal laminae; **E)** bioturbated carbonate mudstone (facies 3) with rare bioclasts; **F)** bioturbated carbonate wackestone (facies 4) containing bioclasts.

4.2 Facies 2 – Bioturbated siliciclastic mudstone with bioclasts

Facies 2 is a dark brown medium siliciclastic mudstone with rare sub-mm scale discontinuous parallel to curved horizontal laminae. The matrix is rich in carbonate, and contains 5 – 10% sub-angular, silt-size quartz grains. The bioturbation index is 3 – 4 (Taylor & Goldring, 1993), and burrows consists of abundant *Chondrites* and *Phycosiphon*-like fecal strings (Figure 4.1C, D). Burrows tend to be elongate and horizontal with silt grains and clay clasts in sub-mm laminae between burrows. Bioclasts (5%) are found scattered randomly throughout this facies; these can be broken or whole, and are generally around 0.5 – 1 mm in length, though rarely up to 8 mm. They are comprised of trilobites, brachiopods, bryozoans, echinoderms, and gastropods. Bioclasts are partially to fully recrystallized and contain abundant pyrite crystals. Pyrite crystals are also preferentially found in the interior fill of burrows.

The extensive *Chondrites* burrows in Facies 2 partially destroys any sedimentary structures present, though sub-mm scale irregular horizontal laminae are still rarely preserved (Figure 4.1D). However, these laminae seem to be superficial, as the grains are aligned between burrows, suggesting that the organisms living in the sediment predominantly changed the fabric of the sediment. The high amount of bioturbation is attributed to both *Chondrites* and the *Phycosiphon*-like fecal strings. This indicates that the conditions at the seafloor must have been at least dysoxic to allow for a moderately diverse benthic life during deposition. The presence of both the silt-size quartz grains as well as relatively frequent outsized bioclasts are here interpreted to reflect bed load processes, in order to transport these from their original location and deposit these grains. However, some bioclasts are whole, and even the fragments are not well abraded, so some of these organisms may have lived in this environment and were transported only short distances.

4.3 Facies 3 – Bioturbated carbonate mudstone

Facies 3 is a light tan carbonate mudstone. Bioclasts (3 – 8%) are fragmented, angular, and randomly oriented. They range from 0.5 – 3mm in length, though most are less than 1mm, and consist of trilobites, brachiopods, bryozoans, and echinoderm fragments. Shell fragments are heavily recrystallized, and contain pyrite crystals as well (Figure 4.1E). It has a bioturbation index of 3 – 4 (Taylor & Goldring, 1993), of *Chondrites* burrows (Figure 4.2A). Burrow orientation is random, and the interior of the burrows have fewer shell fragments than the surrounding sediment, and diagenetic pyrite preferentially occurs in clusters in the interior of the burrows.

Moderate burrowing along with rare bioclasts reflects a low energy, subtidal environment dominated by carbonate deposition. Habitable sea-floor conditions allowed for burrowing to occur, indicating an oxic environment that also preserved burrows. However, the rare, fragmented bioclasts were most likely allochthonous and brought in by shorter episodes of higher energy events. This leads to this facies likely having been relatively undisturbed during deposition, and occurring below normal wave base.

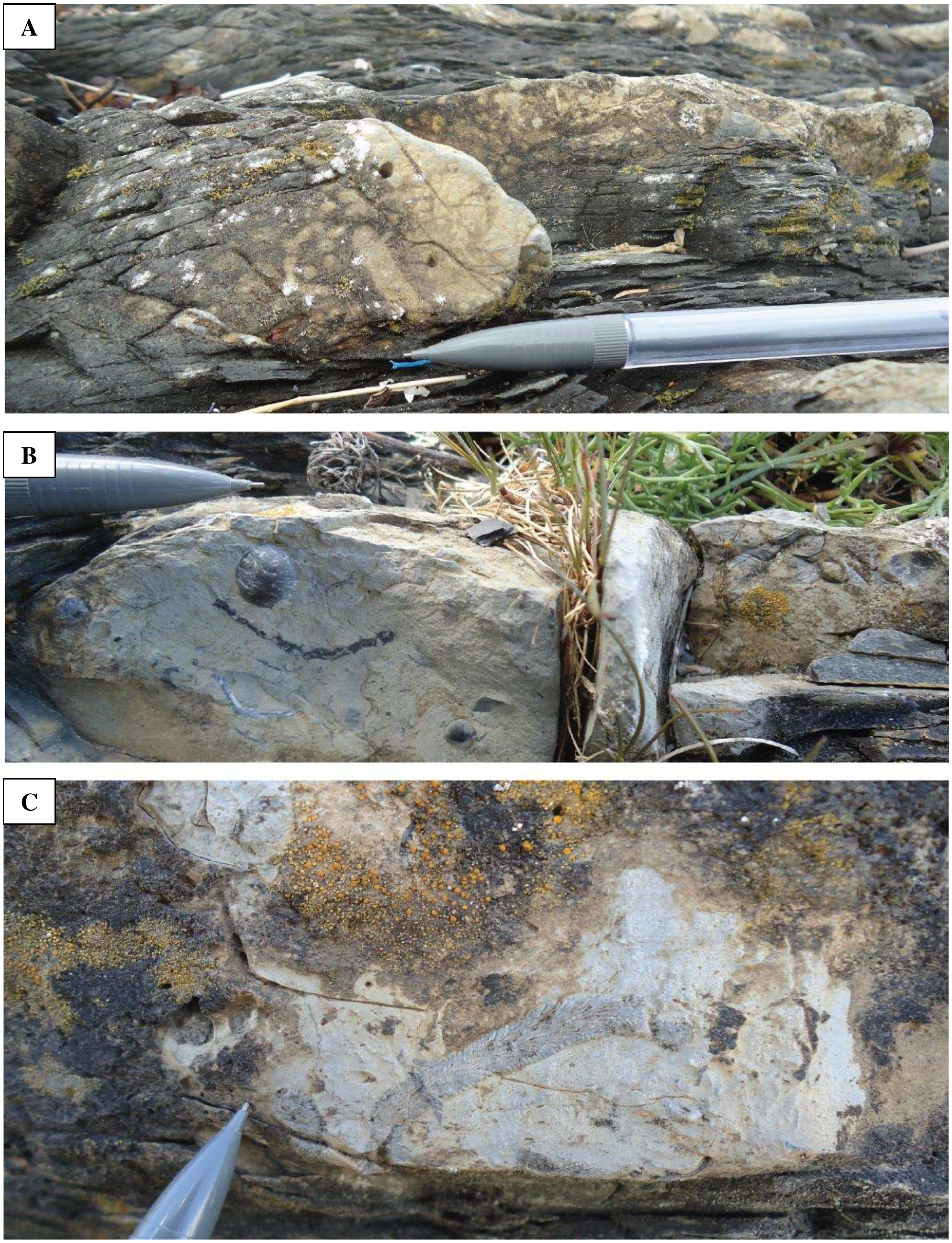

Figure 4.2: Outcrop photos of **A)** *Chondrites* burrows in a carbonate nodule (facies 3); **B)** whole bioclasts (including echinoderms, brachiopods, and trilobites) in a carbonate nodule (facies 4); **C)** a well-preserved bryozoan in a carbonate nodule (facies 4).

4.4 Facies 4 – Bioturbated carbonate wackestone

Facies 4 is a light tan carbonate wackestone. Bioclasts (10 – 20%) are distributed randomly through the facies, and include trilobites, brachiopods, bryozoans, gastropods, and echinoderms. They are moderately to poorly sorted, between 0.5 – 10mm in length, heavily recrystallized, and contain pyrite crystals. The smaller bioclasts tend to be fragmented and angular, while the larger ones are whole (Figure 4.1F, 4.2B, C). Bioturbation index is 4 – 5 (Taylor & Goldring, 1993) of randomly oriented *Chondrites* burrows. This facies rarely shows sub-millimeter wavy horizontal laminae of alternating layers of dark brown silt-sized grains with light tan carbonate grains. These laminae are often disturbed by burrowing, comingling the silt-sized sediment with the surrounding micrite matrix.

Whole, large bioclasts could indicate that some of these organisms were autochthonous and living in the sediment during deposition. Along with the high amount of bioturbation in this facies, this points to abundant benthic life and oxic sea-floor conditions. During these periods, energy levels were low since both burrows and bioclasts are preserved. Still, sub-millimeter wavy horizontal laminae are preserved in this facies, suggesting some bed load transport processes of silt, that was subsequently disturbed by burrowing, and giving it the more wavy appearance. These bed load processes were most likely responsible for bringing in the smaller, fragmented shells as well.

4.5 Facies 5 – Bioclastic packstone

Facies 5 is a carbonate packstone that contains abundant bioclasts (<70%) with a carbonate matrix or siliciclastic mudstone matrix depending on the surrounding sediment type, with silt-sized rounded carbonate fragments. Bioclasts are partially recrystallized and include trilobites, brachiopods, bryozoans, gastropods, and echinoderms, including crinoid stem fragments. Bioclasts range from less than 1 mm up to 11 mm in length, though the majority are 1 – 5 mm in size. In this facies, bioclasts form lenses 2 – 5 cm across, though these lenses can extend up to 10 cm in length (Figure 4.3E, F). Lenses are isolated and tend to be arranged parallel to bedding, though the shells in the lenses are randomly oriented and poorly sorted (Figure 4.4).

The up to several millimeter-size broken bioclasts in this facies reflect a relatively high-energy depositional environment that not only transported these clasts but also caused their fragmentation. Yet, as relatively fragile portions are preserved in some of the bioclasts, such as in bryozoan fragments, the large carbonate grains seem to partially reflect short-distance transport. This facies is seen as a lag deposit that most likely formed during storms or other high-energy events. The silt-size, often rounded carbonate fragments in the matrix, however, indicate that some biogenic detritus must have experienced much longer transport distances leading to significant disintegration and abrasion of the original biogene. The fine grain sizes in the matrix are interpreted as representing the fine-grained sediment load of the depositing flow that settled in between the large carbonate grains, most likely once the flow waned. Still, protected areas, including behind large shell particles, could also have accumulated some of the matrix early during flow.

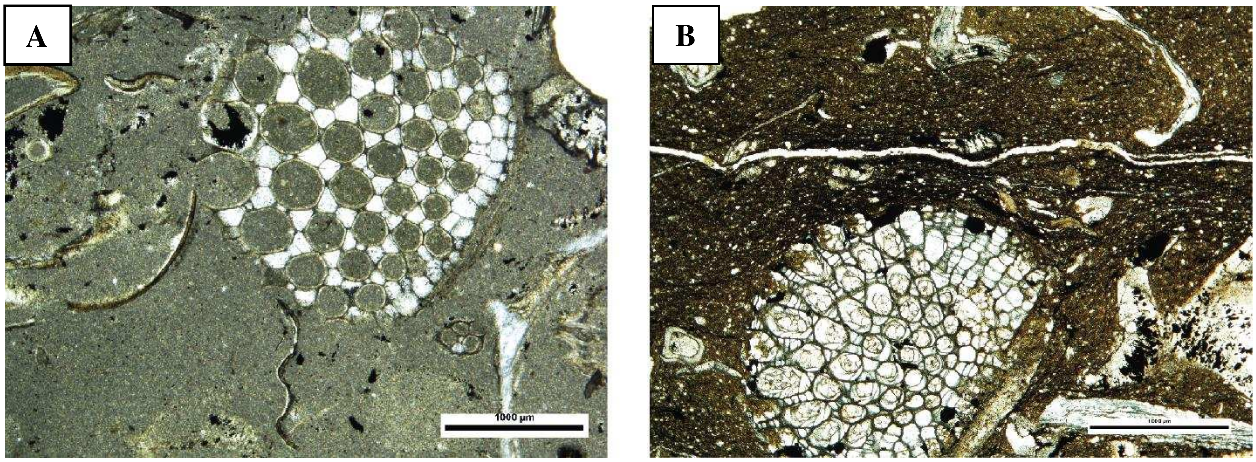

Figure 4.3: Thin section photos of the siliciclastic mudstone and carbonate facies of the Arnestad Formation; scale bar is 1 mm in all photos; **A)** bioclastic packstone (facies 5) surrounded by a carbonate mudstone (facies 4); **B)** bioclastic packstone (facies 5) surrounded by a siliciclatstic mudstone (facies 2).

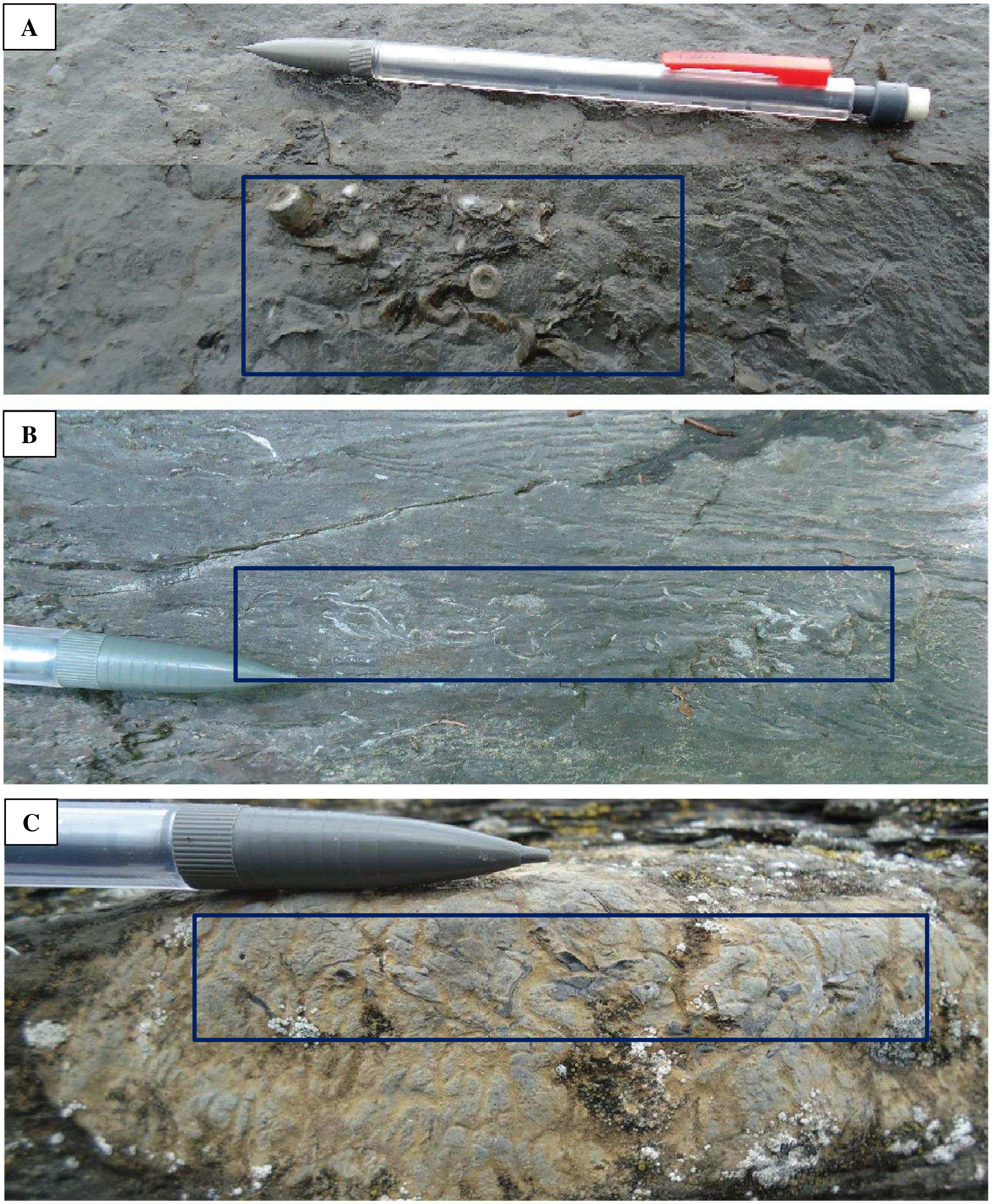

Figure 4.4: Outcrop photos of **A)** fragmented and whole bioclasts (facies 5), including echinoderms, brachiopods, and trilobites, surrounded by a siliciclastic mudstone (facies 1); **B)** fragmented bioclasts (facies 5), including brachiopods and trilobites, surrounded by a fine siliciclastic mudstone (facies 1); **C)** fragmented bioclasts (facies 5), including brachiopods and trilobites, surrounded by a carbonate facies (facies 3).

4.6 Facies 6 – Bioturbated bentonite

Facies 6 consists of blue-green bentonite beds (Figure 4.5) with rare *Chondrites* burrows, with a bioturbation index of 3 (Taylor & Goldring, 1993). The *Chondrites* burrows are filled with a siliciclastic mud matrix, along with very rare bioclast fragments (Figure 4.6A), and looks quite similar to facies 1. Bioclasts are rounded, less than 0.5mm in length, and include brachiopods and trilobites. The bentonite contains angular plagioclase and quartz grains, along with rounded carbonate grains. In some areas, the bentonite has irregular wavy horizontal laminae that is often distorted (Figure 4.6B).

This facies seems to have been deposited in a low energy environment allowing for burrowing to occur undisturbed. Though siliciclastic mud, containing small bioclastic fragments, was transported in order to fill these burrows, energy levels must have still been low enough to not completely rework and destroy this facies and the burrows.

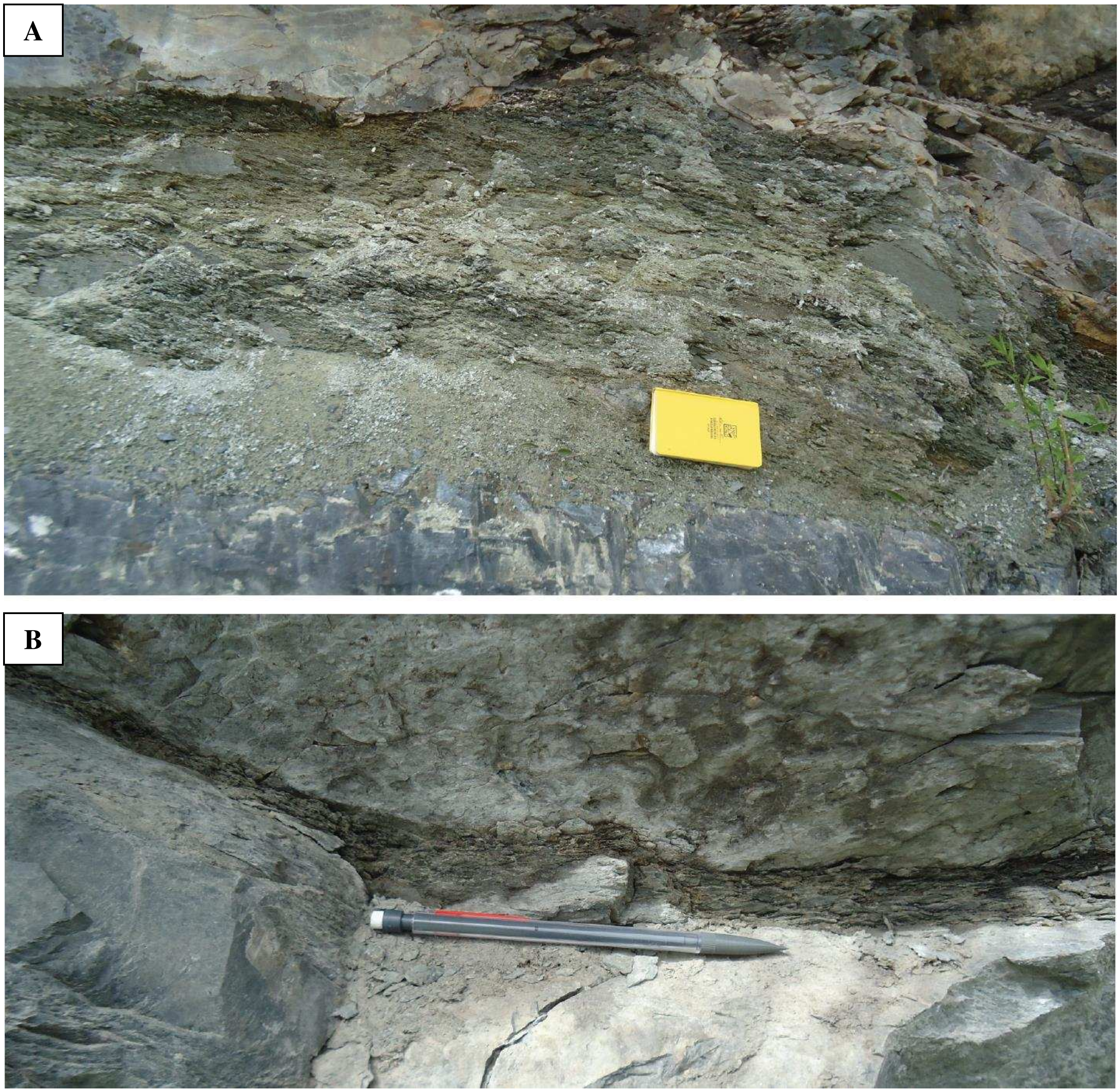

Figure 4.5: Outcrop photos of **A)** the Kinnekulle K-bentonite bed (facies 6) with a thickness of up to 88 cm; **B)** a thin, lenticular bentonite bed (facies 6).

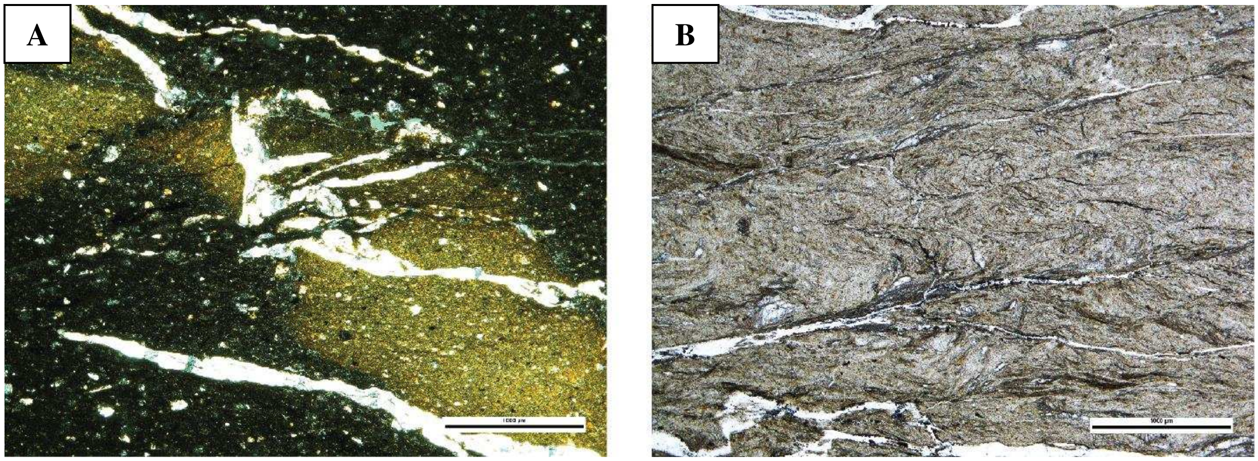

Figure 4.6: Thin section photos of the bentonite beds; **A)** bioturbated bentonite (facies 6) cross-polarized to better show the outline of burrows infilled with fine siliciclastic mudstone (facies 1); **B)** bioturbated bentonite (facies 6) showing contorted laminae.

5.0 FACIES ARCHITECTURE

The Arnestad Formation is approximately 60 m thick in the Oslo-Asker area, described in six measured sections throughout the region (Figure 5.1), yet none encompass the entire formation. Though the Arnestad is characterized by repetitive deposition of siliciclastic mudstones and carbonate nodules, there are variations in these ratios throughout the section. The Arnestad Formation in this study is divided into three stratigraphic intervals based on the relationship and depositional changes between the siliciclastic mudstones and carbonate beds.

The Lower Arnestad Formation includes the bottom 9 m of the formation (9 m mark on the Bekkebukta section; 4.5 m mark on the Vollen section) and is dominated by bioclastic carbonate nodules (Facies 3, 4) interbedded with siliciclastic mudstones (Facies 1, 2). Siliciclastic mudstones range in thickness from 5 – 29 cm, with most beds around 10 – 14 cm thick. Carbonate nodules form mostly continuous beds and are typically 2 – 5 cm thick, but range from 1 – 7 cm in thickness. Carbonate beds are also often found in packages of 2 – 3 with 0.5 – 3 cm of siliciclastic mudstone in between. In outcrop, *Chondrites* burrows are visibly apparent in all of the carbonate beds, while shell fragments are mostly unidentifiable, and rarely echinoderms, brachiopods, and gastropods can be recognized (Facies 5).

The Middle Arnestad Formation comprises the overlying 36 m of the formation (includes all of the Elnestangen section, and the upper boundary is defined by the 5m mark on the Robben section, and 13m mark on the Bentonite Arnestad section) and is composed mostly of siliciclastic mudstones (Facies 1, 2) that are interbedded with carbonate nodule beds (Facies 3,4). Mudstones range in thickness from 14 – 64 cm and are typically 22 – 36 cm thick. Carbonate nodules are mostly discontinuous, and range in thickness from 1 – 8 cm, with most around 2 – 5 cm thick. Similar to the Lower Arnestad Formation, *Chondrites* burrows are visible in outcrop throughout the section in the carbonates, along with unidentifiable shell fragments, though both are not as apparent. However, in the upper 10m of the Middle Arnestad, the siliciclastic mudstones rarely contain shell fragments, and, if present, only in unsorted lenses (Facies 5). This section also has ash layers (Facies 6) in lenses, 0.5 – 3 cm thick and 1 – 10's of meters wide. These beds occur infrequently, and thin out on their margins. One notably large bed, known as the Kinnekule K-bentonite bed is up to 88 cm thick and is found in the upper part of this section.

The Upper Arnestad Formation is 15 m thick, and is dominated by siliciclastic mudstones (Facies 1, 2) interbedded with carbonate nodules (Facies 3, 4) arranged in packages of multiple layers. The siliciclastic mudstones range from 19 – 88 cm in thickness, with most beds typically 35 – 50 cm thick. The carbonate nodules are mostly discontinuous along the bed, range from 3 – 11 cm in thickness, but are typically 3 – 4 cm thick. The carbonate nodules are often arranged in packages of two to three beds, separated by 0.5 – 6 cm of siliciclastic mudstone. *Chondrites* burrows are abundant in the carbonate nodules and visible in outcrop, and burrows into the surrounding mudstone can be seen in places. Throughout the Upper Arnestad Formation, broken shell fragments are found in all the beds, and are often accumulated in unsorted lenses (Facies 5), that increase in frequency of occurrence upwards through the formation.

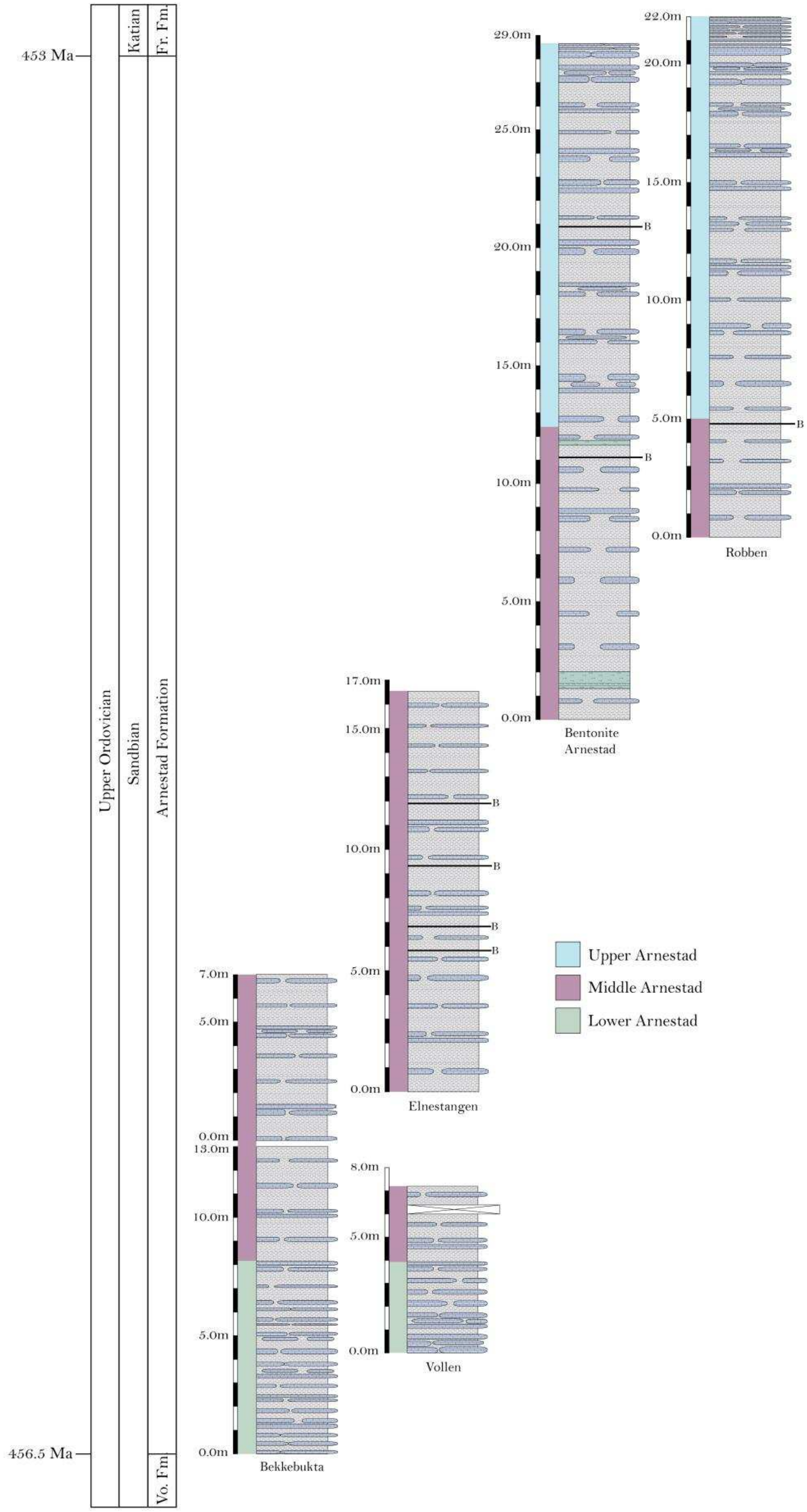

Figure 5.1: Correlated measured sections of the Arnestad Formation at 5 different localities. Contacts with the Vollen Formation (Vo. Fm.) and Frognerkilen Formation (Fr. Fm) are shown, along with approximate age based on Svensen et al., (2015), and Cooper and Sadler, (2012).

6.0 DEPOSITIONAL MODEL

During the Ordovician, the Baltica terrane had low relief (Bjørlykke, 1974b), and was covered by an overall shallow epicontinental sea (Bruton et al., 1985). This gentle morphology facilitated the development of the Arnestad Formation as a carbonate ramp system with a lithologically clear distinction into two broad facies belts (Figure 6.1). These facies belts are reflected in the facies types: carbonates characterized the proximal, but not shallow-marine, depositional zone equivalent to the middle and outer ramp of Buchette and Wright (1992), whereas towards the distal deep shelf environment exclusively siliciclastic mudstones were deposited (“basin setting” of Burchette and Wright, 1992).

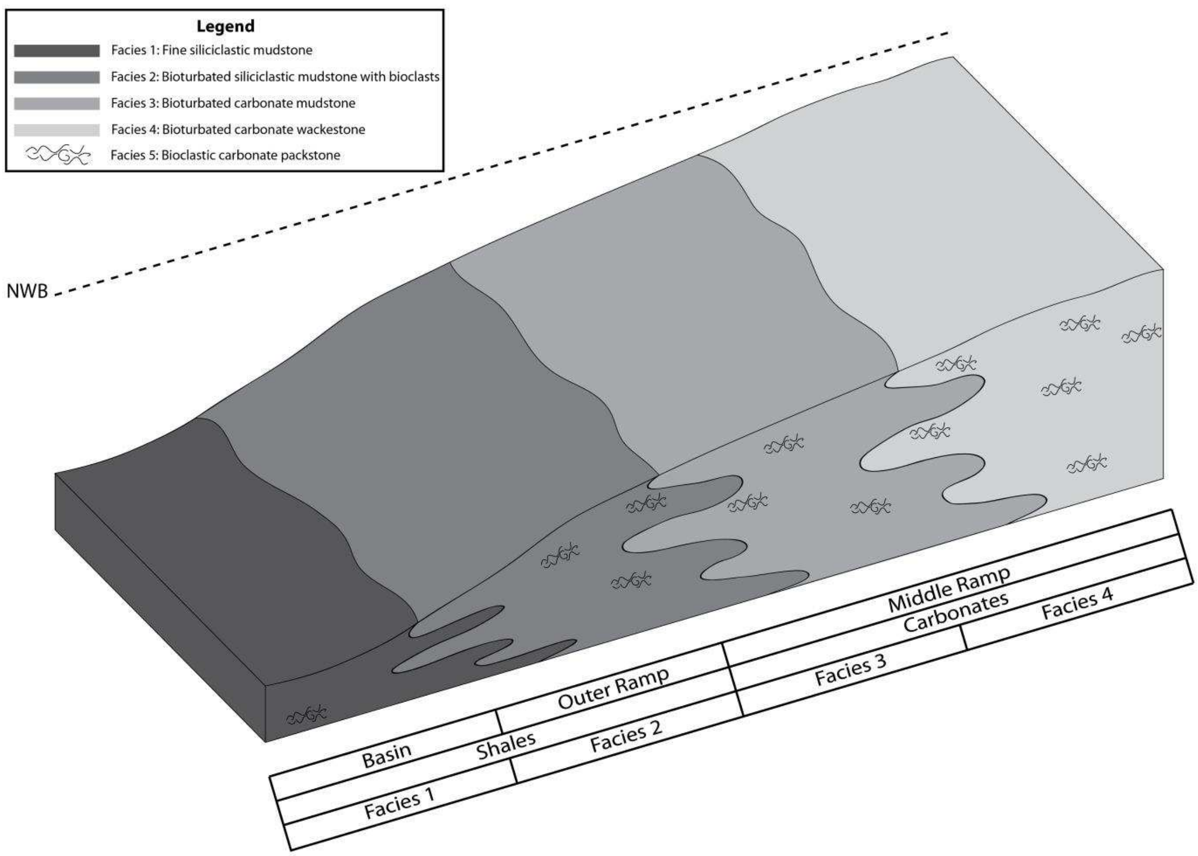

Figure 6.1: Depositional model characterizing the Arnestad Formation on a carbonate ramp system, with siliciclastic mudstone deposited more distally (facies 1 and 2), and carbonates deposited more proximally (facies 3 and 4). Normal wave base (NWB) is represented by the dashed line.

The shallowest facies on this carbonate ramp is represented by the bioturbated carbonate wackestones (facies 4), with some intercalated facies 5 bioclastic packstones. This facies co-occurrence likely represents a mid-ramp setting with the wackestones reflecting fair-weather conditions while the packstones mirror the effect of high-energy events such as storms. The amount and variety of fossils indicates that abundant organisms were living on and in the sediment during fair weather. During storms, however, the high energy concentrated the shells, and deposited them preferentially in scours eroded into the ocean floor. The micrite, ubiquitous in facies 4, is not quite as common in facies 5 and must have been incorporated into the packstones during the last waning stages of the storm.

The wacke- and packstones of facies 4 and 5 grade distally into a facies belt comprised of the mudstones and packstones of facies 3 and 5. This zone is located basinwards of the facies 4 and 5 carbonates, where fair weather sedimentation mostly accumulated micrite with only minor amounts of carbonate grains, and including just remnants of organisms that are thought to live in this setting. Storms, however, had a similar effect on facies 3 as on facies 4; it accumulated and likely broke some of the shells in lags, and concentrated them in irregular laminae and scours on the sea floor.

Seaward of the carbonate facies zones, the Arnestad depositional system showed two siliciclastic mudstone facies belts: the proximal bioturbated siliciclastic mudstone with bioclasts (facies 2), and the distal fine siliciclastic mudstone (facies 1). The proximal siliciclastic mudstone facies reflects the adjacent carbonates with abundant micrite in the matrix as well as the presence of carbonate bioclasts. This proximal shale facies belt must have received abundant carbonate mud from nearshore environments, yet also shows significant siliciclastic silt and mud settling, indicating an offshore "basinal" setting (cf. Burchette and Wright, 1992). The carbonate bioclasts support the presence of currents that could transport up to silt-size grains from carbonate environments located closer to the coast downslope. The same currents may also be partly responsible for carrying the carbonate mud into the proximal offshore realm.

The most distal facies belt of the Arnestad depositional system was characterized by the fine siliciclastic mudstones of facies 1. The siliciclastic mud in this offshore facies belt was deposited in an environment that portrayed abundant benthic life; ultimately the amount of burrowing overprinted any sedimentological structure that may have been present originally in this setting. It is here speculated that the carbonate was introduced into this environment by offshore-directed currents (?) transporting carbonate mud, while the siliciclastic mud represents terrigenous run-off. Some bed-load transport is reflected in the rounded nature of the bioclasts, indicating that advective transport of silt-size particles, likely during high-energy events such as storms, did play a role in this environment.

The facies architecture of the Arnestad Formation reveals two orders of intercalations of contrasting facies here interpreted to represent cycles of different orders. The small-scale cycles are represented by the interbedding of up to decimeter-thick mudstones with centimeter-thick carbonates. These cycles reflect small-scale sea-level changes and the transitional shift between proximal carbonate and distal siliciclastic mudstone deposition. The large-scale cycles are represented by the stratigraphic changes over the entire formation and separated into the lower, middle, and upper portions of the Arnestad Formation. The lower Arnestad Formation contains a fairly equal amount of siliciclastic mudstones and carbonate beds, and indicates a relatively low sea-level position. Sea-level shifts to an overall high sea-level stand during the middle Arnestad, as it is dominated by siliciclastic mudstones with carbonate beds occurring less frequently. In the upper Arnestad Formation, thick siliciclastic mudstone beds with intercalated layers of carbonate and thin siliciclastic mudstones suggest another sea-level low stand.

7.0 DISCUSSION

7.1 Carbonate deposition and diagenesis

The Arnestad Formation is composed of bioturbated carbonate mudstones and wackestones, intercalated with siliciclastic mudstones, interpreted as being deposited on an epicontinental ramp system. This study suggests that the carbonate is a result of primary deposition, and even though the carbonate beds often resemble concretionary beds, e.g. as described by Jenkyns (1974) for the Jurassic of the Mediterranean region, they are not a product of diagenesis.

The main argument for the carbonates representing primary mud-rich deposits is that the micrite is well preserved in many of the samples, and even though it may be partly recrystallized in places, it still shows grains that are oriented in different positions demonstrating primary deposition. While carbonate concretions often form individual lens-shaped nodules along bedding planes, many of the mud-rich carbonates in the Arnestad Formation are exposed as continuous beds, reflecting its primary origin. Nevertheless, no distinct bedding planes or other sedimentary features have been observed in the mudstones in the Arnestad Formation, making it more likely for these carbonate beds to be deposited, rather than formed by precipitation of carbonate in siliciclastic mudstone pore spaces.

7.2 Cyclicity and sea-level changes

At a basic level, the average length of one cycle in the Arnestad Formation can be estimated roughly by dividing the approximate duration of the Arnestad by the total amount of cycles documented in this unit. It is estimated that the Arnestad Formation was deposited over a time period of ~3.5 my (Cooper and Sadler, 2012), and contains between 215 – 220 cycles. This puts each cycle at an average duration between 15,900 and 16,300 years. These values are consistent with Milankovitch-type precessional cycles for they are in the generally accepted range of 16,400 – 23,000 years (Berger and Loutre, 1994).

However, both the number of cycles as well as the absolute duration of the Arnestad Formation can only be approximately defined. The number of graptolites and other time indicative biostratigraphic fossils are not conclusive and therefore, the unit may represent slightly more or less time than the 3.5 my envisioned by Cooper and Sadler (2012). Similarly, the number of cycles in the Arnestad Formation may not be 215 – 220 cycles but significantly more (or less) than assumed in this study. The succession used in this study to show the entire formation, and which the cycle numbers are based on, is composed of several correlated section pieces. These correlations are based on only lithological arguments. From that standpoint, even though the correlations are done with the best of our knowledge, they still could be flawed, and result in the assumption of a significantly thicker or thinner unit than presented in this study.

Even assuming that the correlations are largely correct, some cycles may not be visible in the field because of a lack of lithological contrast between successive cycles. The fact that an intercalation of carbonates resembled a cycle but is indeed caused by a different process such as a severe storm could also bias the amount of cycles counted. The presented numbers of approximately 16,000 years per cycle therefore characterize an order of magnitude that these cycles presumably represent, and the ones in the Arnestad Formation are most likely Milankovitch cycles in the precession band.

Precessional cycles have been reported from several other carbonate environments (e.g. Goldhammer et al., 1987; Strasser, 1994; Zühlke et al., 2003) but most importantly occur in a mostly carbonate unit underlying the Arnestad Formation in the Oslo area, and Arnestad-equivalent strata throughout southern and central Sweden (Bruton et al., 1985). The early

Ordovician Bjørkåsholmen Formation is reported by Egenhoff et al. (2010) to contain up to 11 small-scale cycles, also interpreted as sediment patterns reflecting precession. If both the Arnestad and the Bjørkåsholmen Formation show the same cycle type, it is most likely that precessional control on sedimentary patterns was very strongly developed throughout large parts of the Ordovician, especially on the Baltica microplate.

7.3 Volcanic activity and ash deposition

The Arnestad Formation contains several ash beds that are concentrated in the upper portion of the middle part of the unit, and signal volcanic eruptions, likely from a volcanic arc system related to the subduction of the Iapetus Ocean below Baltoscandia (cf. Cocks and Torsvik, 2005). Nevertheless, it remains unclear why ashes are almost exclusively preserved in this one stratigraphic interval and not throughout this unit, as the arc system was likely active during the entire time-span the Arnestad Formation was deposited.

The middle part of the Arnestad Formation contains less carbonate intervals than both the upper and lower part of this unit. Following the depositional model presented in this study, this presumably indicates a slightly deeper depositional environment containing less of the slightly shallower-marine carbonate intercalations. An overall deeper environment would also be characterized by lower energy conditions. Preserving ash beds, thick or thin, would therefore be more likely in an environment containing more siliciclastic mudstones than in one that is rich in carbonates. In that respect, the abundance of ash beds in the upper part of the siliciclastic mudstone-dominated middle Arnestad Formation is to be expected as the predominance of low energy conditions probably promoted the preservation of ash beds.

However, the lower and central part of the middle Arnestad Formation show equally low energy conditions as the upper middle portion, yet they do not contain any ash beds. This apparent contradiction may be explained by changes in the intensity and frequency of volcanic eruptions (Huff et al., 2010), and the resulting lack of deposition of ash beds during deposition of the early and central middle Arenstad Formation, likely during times of volcanic quiescence. Variations in ash production are even noticeable during upper middle Arnestad times when both thin as well as one very thick ash beds were deposited. Ultimately, ash beds may also not always be preserved well, especially for thin ash beds in relatively deep shelf environments.

Entirely bioturbated ash beds can be seen in the thin ashes preserved in the Arnestad Formation (Figure 4.5) and mixing ash components with the underlying (and overlying?) mudstone beds. It therefore seems reasonable to assume that the Arnestad Formation may actually record higher amounts of ash deposition that could not be recognized in outcrop because they were largely equivalent to the surrounding mudstone from intense bioturbation. Also, considering that the ash beds reflect the volcanism of an approaching arc, it would seem reasonable to assume that the upper middle Arnestad Formation contains higher amounts of ash beds instead of the lower Arnestad Formation, when the arc was still further away from Baltoscandia. Therefore, there may still be undiscovered very thin ash beds in the lower part of the middle Arnestad Formation that could be recognized in excellent and especially fresh outcrops. They would, however, likely thoroughly bioturbated, and it is unclear how much they are mixed in with the surrounding lithology.

8.0 CONCLUSIONS

1. The Arnestad Formation contains six facies: two siliciclastic mudstone facies, three carbonate facies, and one bentonite facies. These are: 1) fine siliciclastic mudstone, 2) bioturbated siliciclastic mudstone with bioclasts, 3) bioturbated carbonate mudstone, 4) bioturbated carbonate wackestone, 5) bioclastic packstone, and 6) bioturbated bentonite. All facies show some amount of bioturbation, and, except for the bentonite (facies 6), contain whole and/or fragmented bioclasts.
2. This study is based on six detailed measured sections, each one characterizing one or more parts of the succession. According to these sections, the Arnestad Formation consists of three stratigraphic intervals, divided based on the relative amount of siliciclastic mudstone and carbonate beds. The lower Arnestad Formation is dominated by bioclastic carbonate beds of facies 3 and 4; the middle Arnestad Formation contains mostly siliciclastic mudstone beds (facies 1 and 2) and ash layers (facies 6), with few carbonate beds (facies 3 and4); and the upper Arnestad Formation shows thick beds of siliciclastic mudstones (facies 1 and 2) interbedded with continuous nodular carbonate beds (facies 3 and 4) that are arranged in packages of 2 – 3 beds, and separated by several centimeters of siliciclastic mudstone. Correlation of the six sections estimates the overall thickness for the Arnestad Formation at about 60 m.
3. The sedimentary system of the Arnestad Formation encompasses the middle to outer ramp areas and basin, depositing siliciclastic mud distally, and micrite more proximally. All facies are interpreted as being deposited below normal wave base, and most likely below effective storm wave base. Facies 5, interpreted as representing storm influences on deposition, is present in conjunction with all the other facies, but increases in abundance upwards through

the formation. Bioturbated carbonate wackestones (facies 4) is the shallowest facies on a mid-ramp setting grading basinward into the bioturbated carbonate mudstone of facies 3. Seaward of the carbonate facies belts is the proximal bioturbated siliciclastic mudstone with bioclasts (facies 2) found in the outer-ramp, while the most distal facies of fine siliciclastic mudstones (facies 1), was deposited in the basin. Bed load processes likely influenced deposition in all facies, and were responsible for transporting sediment and bioclasts basinwards.

4. Even though many of the carbonate beds in the Arnestad resemble bed-parallel concretions, the amount of primary micrite they contain indicates that they are primary in origin and only diagentically overprinted.
5. The intercalation between siliciclastic mudstones and carbonate beds throughout the Arnestad Formation is interpreted to indicate cyclical forcing. Cycle duration is between 15,900 and 16,300 years, and is therefore tentatively interpreted as representing Milankovitch precessional frequencies.
6. The middle Arnestad Formation contains several ash beds which likely originated from volcanic activity to the northwest. This study envisioned that the middle Arnestad environment most likely promoted the preservation of ashes as it represents the most distal and quietest of all three sub-units. All ash beds are bioturbated, rendering the beds more difficult to recognize because of their similarity to the surrounding rock. Therefore, more ash beds may have been deposited in this unit than hitherto recognized because of the intense bioturbation.

9.0 REFERENCES

Algeo, T.J., Marenco, P.J., and Saltzman, M.R., 2016, Co-evolution of oceans, climate, and the biosphere during the ‘Ordovician Revolution’: A review, Palaeogeography, Palaeoclimatology, Palaeoecology, v. 458, p. 1 – 11.

Berger, A., Loutre, M.F., 1994, Astronomical forcing through geological time, *in* de Boer, P.L., Smith, D.G. eds, Orbital forcing and cyclic sequences, IAS Special Publication, v. 19, p. 15 – 24.

Bergström, S.M., Huff, W.D., Kolata, D.R., and Bauert, H., 1995, Nomenclature, stratigraphy, chemical fingerprinting, and areal distribution of some Middle Ordovician K-bentonites in Baltoscandia, GFF, v. 117, p. 1 – 13.

Bjørlykke, K. 1974a. Depositional history and geochemical composition of lower Paleozoic epicontinental sediments from the Oslo Region, Norway, Norges Geologiske Undersøkelse Bulletin 305, 81 pp.

Bjørlykke, K., 1974b, Geochemical and mineralogical influence of Ordovician Island Arcs on epicontinental clastic sedimentation: a study of Lower Palaeozoic sedimentation in the Oslo Region, Norway, Sedimentology, v. 21, p. 251 – 272.

Borcovsky, D., Egenhoff, S., Fishman, N., Maletz, J., Boehlke, A., and Lowers, H., 2017, Sedimentology, facies architecture, and sequence stratigraphy of a Mississippian black mudstone succession – The upper member of the Bakken Formation, North Dakota, United States, AAPG Bulletin, v. 101, no. 10, p. 1625 – 1673.

Bruton, D.L., Lindstrom, M., and Owen, A.W., 1985, The Ordovician of Scandinavia, *in* Gee, D.G., and Sturt, B.A. eds, The Caledonide Orogen – Scandinavia and related areas, John Wily, Chichester, p. 273 – 282.

Bruton, D.L., Gabrielsen, R.H., and Larsen, B.T., 2010, The Caledonides of the Oslo Region, Norway – stratigraphy and structural elements, Norwegian Journal of Geology, v. 90, p. 93 – 121.

Burchette, T.P., and Wright, V.P., 1992, Carbonate ramp depositional systems, Sedimentary Geology, v. 79, p. 3 – 57.

Cocks, L.R., and Torsvik, T.H., 2005, Baltica from the late Precambrian to mid-Palaeozoic times: the gain and loss of a terrane’s identity, Earth Science Reviews, v. 72, p. 39 – 66.

Cooper, R.A., and Sadler, P.M., 2012, The Ordovician Period, *in* Gradstein, F.M., Ogg, J.G., Schmitz, M.D., and Ogg, G.M., eds, The geologic time scale 2012, Elsevier, Oxford, United Kingdom, p. 489 – 523.

Egenhoff, S., Cassle, C., Maletz, J., Frisk, A.M., Ebbestad,Stübner, K., 2010, Sedimentology and sequence stratigraphy of a pronounced Early Ordovician sea-level fall on Baltica – the Bjørkåsholmen Formation in Norway and Sweden, Sedimentary Geology, v. 224, p. 1 – 14.

Egenhoff, S.O., Fishman, N.S., Ahlberg, P., Maletz, J., Jackson, A., Kolte, K., Lowers, H., Mackie, J., Newby W., and Ptrowsky, M., 2015, Sedimentology of SPICE (Steptoean positive carbon isotope excursion): A high-resolution trace fossil and microfabirc analysis of the middle to late Cambrian Alum Shale Formation, southern Sweden, *in* Larsen, D., Egenhoff, S.O., and Fishman N.S., eds., Paying attention to mudrocks: Priceless!, Geological Society of America Special Paper 515, p. 87 – 102.

Goldhammer, R.K., Dunn, P.A., Hardie, L.A., 1987, High frequency glacio-eustatic sea level oscillations with Milankovitch characteristics recorded in Middle Triassic platform carbonates in northern Italy, American Journal of Science, v. 287, p. 853 – 892.

Google, 2016, Oslo, Norway region, retrieved September 25, 2016, from https://goo.gl/BRhgrd.

Grahn, Y., and Nõlvak, J., 2007, Remarks on older Ordovician Chitinozoa and biostratigraphy of the Oslo Region, southern Norway, GFF, v. 129, p. 101 – 106.

Greiling, R.O., and Garfunkel, Z., 2007, An Early Ordovician (Finnmarkian?) foreland basin and related lithospheric flexure in the Scandinavian Caledonides, American Journal of Science, v. 307, p. 527 – 553.

Hansen, J., and Harper, D.A.T., 2008, The late Sandbian – earliest Katian (Ordovician) brachiopod immigration and its influence on the brachiopod fauna in the Oslo Region, Norway, Lethaia, v. 41, p. 25 – 35.

Hansen, J., Nielsen, J.K., and Hanken, N., 2009, The relationships between Late Ordovician sea-level changes and faunal turnover in western Baltica: Geochemical evidence of oxic and dysoxic bottom-water conditions, Palaeogeography, Palaeoclimatology, Palaeoecology, v. 271, p. 268 – 278.

Huff, W.D., Bergström, S.M., and Kolata, D.R., 2010, Ordovician explosive volcanism, *in* Finney, S.C., and Berry, W.B.N. eds, The Ordovician Earth System, Geological Society of America Special Paper, v. 466, p. 13 – 28.

Lazar, O.R., Bohacs, K.M., Macquaker, J.H.S., Schieber, J., and Demko, T.M., 2015, Capturing key attributes of fine-grained sedimentary rocks in outcrops, cores, and thin sections: Nomenclature and description guidelines, Journal of Sedimentary Research, v. 85, p. 230 – 246.

Macquaker, J.H.S., and Adams, A.E., 2003, Maximizing information from fine-grained sedimentary rocks: and inclusive nomenclature for mudstones, Journal of Sedimentary Research, v. 73, no. 5, p. 735 – 744.

Macquaker, J.H.S., and Bohacs, K.M., 2007, On the accumulation of mud, Science, v. 318, no. 5857, p. 1734 – 1735.

Macquaker, J.H.S., Bentley, S.J., and Bohacs, K.M., 2010, Wave-enhanced sediment-gravity flows and mud dispersal across continental shelves: Reappraising sediment transport processes operating in ancient mudstone successions, Geological Society of America, v. 38, no. 10, p. 947 – 950.

Munnecke, A., Calner, M., Harper, D.A.T., and Servais, T., 2010, Ordovician and Silurian sea-water chemistry, sea level, and climate: A synopsis, Palaeogeography, Palaeoclimatology, Palaeoecology, v. 296, p. 389 – 413.

Nielsen, A.T., 2004, Ordovician sea level changes: A Baltoscandian Perspective, *in* Webby, B.D., Paris, F., Droser, M.L., and Percival, J.G., eds., The Great Ordovician Biodiversification Event: New York, Columbia University Press, p. 84 – 93.

Owen, A.W., Bruton, D.L., Bockelie, J.F., and Bockelie, T.G., 1990, The Ordovician successions of the Oslo Region, Norway, Norges Geologiske Undersøkelse Special Publication 4, p. 3 – 54.

Schieber, J., 1998, Deposition of mudstones and shales: overview, problems, and challenges, *in* Schieber, J., Zimmerle, W., and Sethi, P.S., eds., Shales and Mudstones, Volume I, Stuttgart, E. Schweizerbarth'sche Verlagsbuchhandlung, p. 131 – 146.

Schieber, J., Southard, J., and Thaisen, K., 2007, Accretion of mudstone beds from migrating floccule ripples, Science, v. 318, p. 1760 – 1763.

Schieber, J., and Yawar, Z., 2009, A new twist on mud deposition – mud ripples in experiment and rock record, The Sedimentary Record, v. 7, no. 2, p. 4 – 8.

Schieber, J., 2016, Mud re-distribution in epicontinental basins – Exploring likely processes, Marine and Petroleum Geology, v. 71, p. 119 – 133.

Størmer, L., 1953, The Middle Ordovician of the Oslo Region, Norway: 1. Introduction to stratigraphy, Norsk Geologisk Tidsskrift, v. 31, p. 37 – 141.

Strasser, A., 1994, Milankovitch cyclicity and high-resolution sequence stratigraphy in lagoonal – peritidal carbonates (Upper Tithonian – Lower Berriasian, French Jura Mountains), *in* de Boer, P.L., Smith, D.G. eds, Orbital forcing and cyclic sequences, IAS Special Publication, v. 19, p. 285 – 301.

Svensen, H.H., Hammer, O., and Corfu, F., 2015, Astronomically forced cyclicity in the Upper Ordovician and U-Pb ages of interlayered tephra, Oslo Region, Norway, Palaeogeography, Palaeoclimatology, Palaeoecology, v. 418, p. 150 – 159.

Taylor, A.M., and Goldring, R., 1993, Description and analysis of bioturbation and ichnofabric, Journal of the Geological Society, London, v. 150, p. 141 – 148.

Trotter, J.A., Williams, I.S., Barnes, C.R., Lécuyer, C., Nicoll, R.S., 2008. Did cooling oceans trigger Ordovician biodiversification? Evidence from conodont thermometry, Science, v. 321, p. 550 – 554.

Zühlke, R., Bechstädt, T., and Mundil, R., 2003, Sub-Milankovitch and Milankovitch forcing on a model Mesozoic carbonate platform – the Latemar (Middle Triassic, Italy), Terra Nova, v. 15, p. 69 – 80.

10.0 APPENDICES

Appendix 1: Expanded correlated measured sections of the Arnestad Formation at 5 different localities.

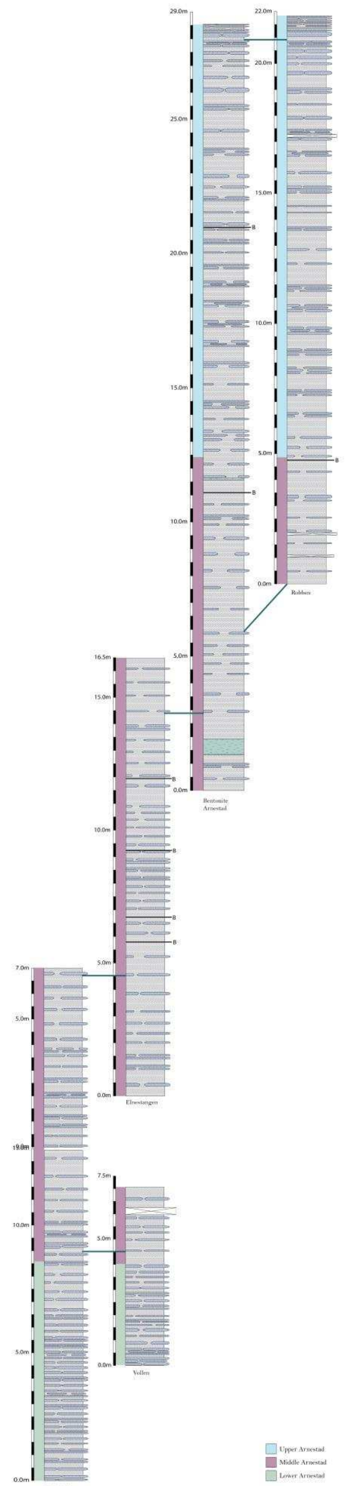

Appendix 2: Original measured sections of the Arnestad Formation

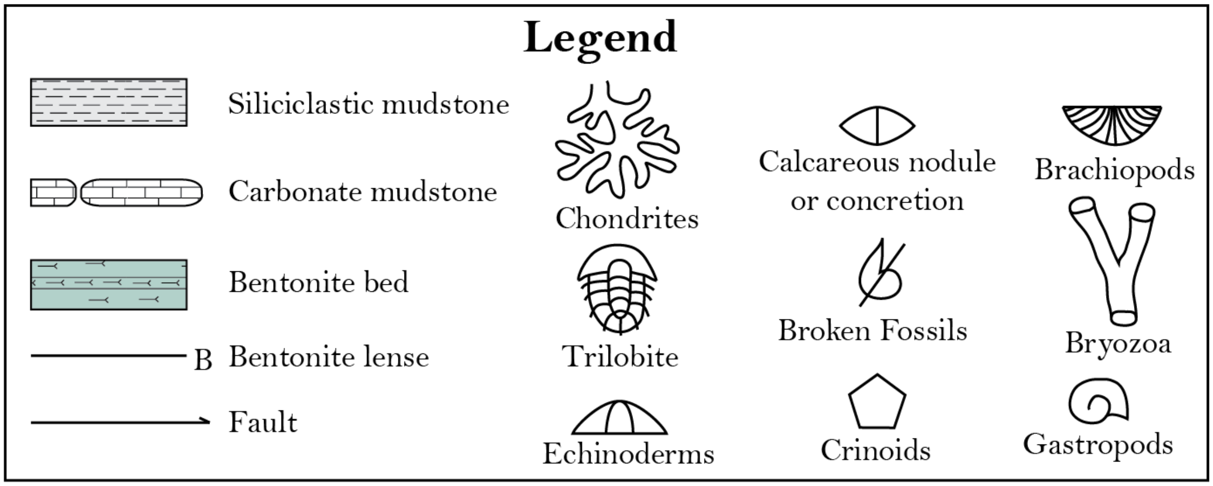

Appendix 2.1: Bekkebukta measured section

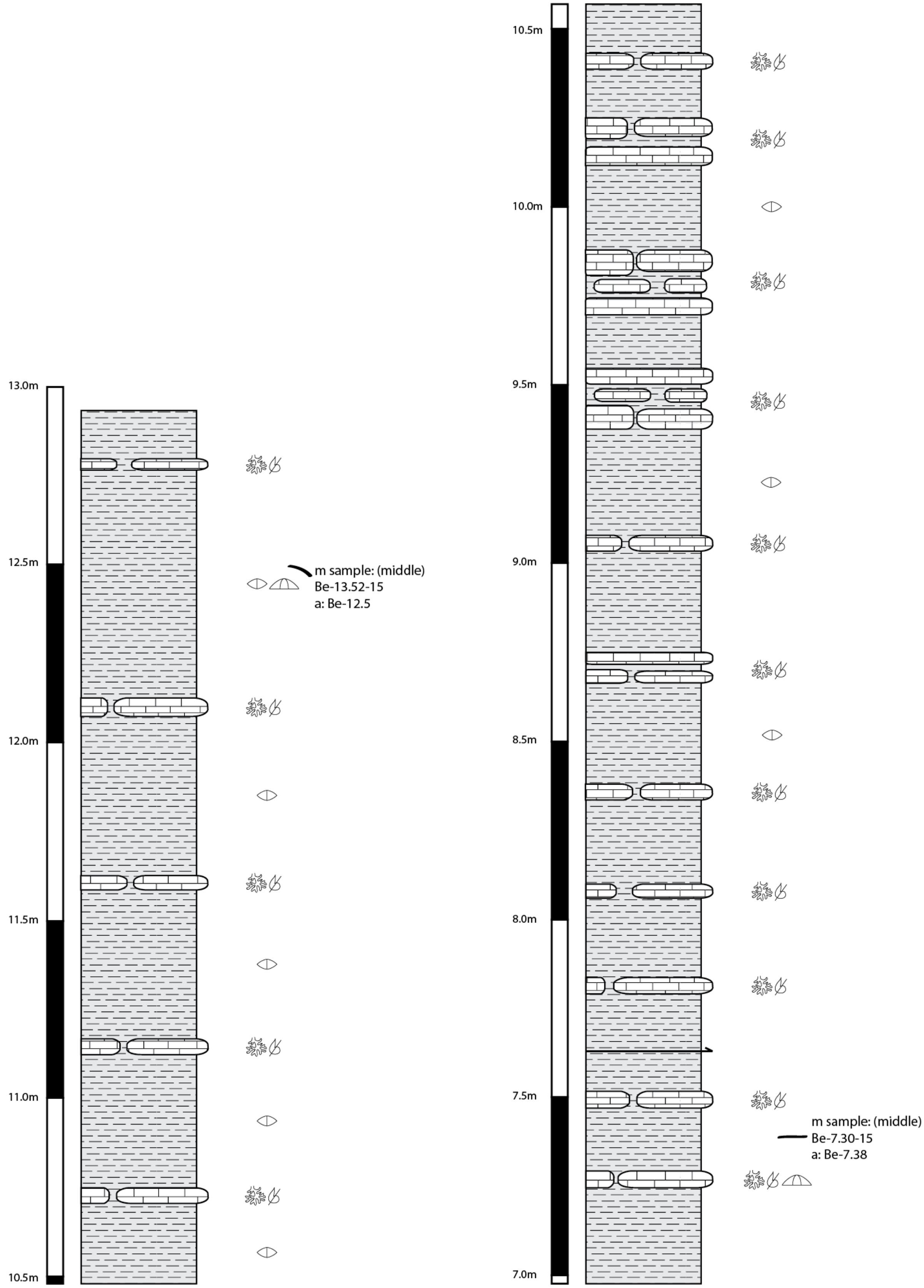

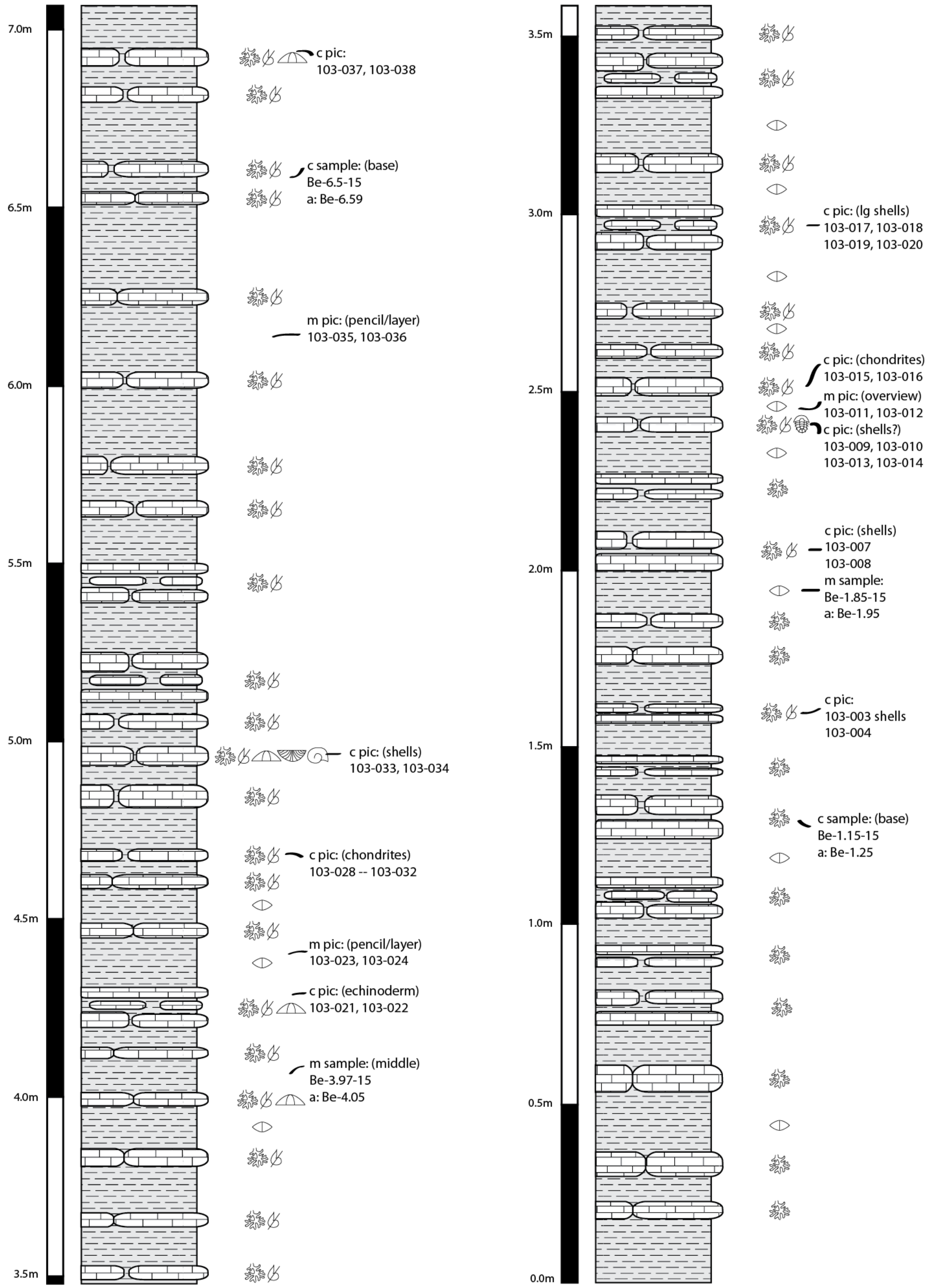
7.0m
6.5m
6.0m
5.5m
5.0m
4.5m
4.0m
3.5m
c pic:
103-037, 103-038
c sample: (base)
Be-6.5-15
a: Be-6.59
m pic: (pencil/layer)
103-035, 103-036
c pic: (shells)
103-033, 103-034
c pic: (chondrites)
103-028 -- 103-032
m pic: (pencil/layer)
103-023, 103-024
c pic: (echinoderm)
103-021, 103-022
m sample: (middle)
Be-3.97-15
a: Be-4.05
3.5m
3.0m
2.5m
2.0m
1.5m
1.0m
0.5m
0.0m
c pic: (lg shells)
103-017, 103-018
103-019, 103-020
c pic: (chondrites)
103-015, 103-016
m pic: (overview)
103-011, 103-012
c pic: (shells?)
103-009, 103-010
103-013, 103-014
c pic: (shells)
103-007
103-008
m sample:
Be-1.85-15
a: Be-1.95
c pic:
103-003 shells
103-004
c sample: (base)
Be-1.15-15
a: Be-1.25

Appendix 2.2: Bekkebukta 2 measured section

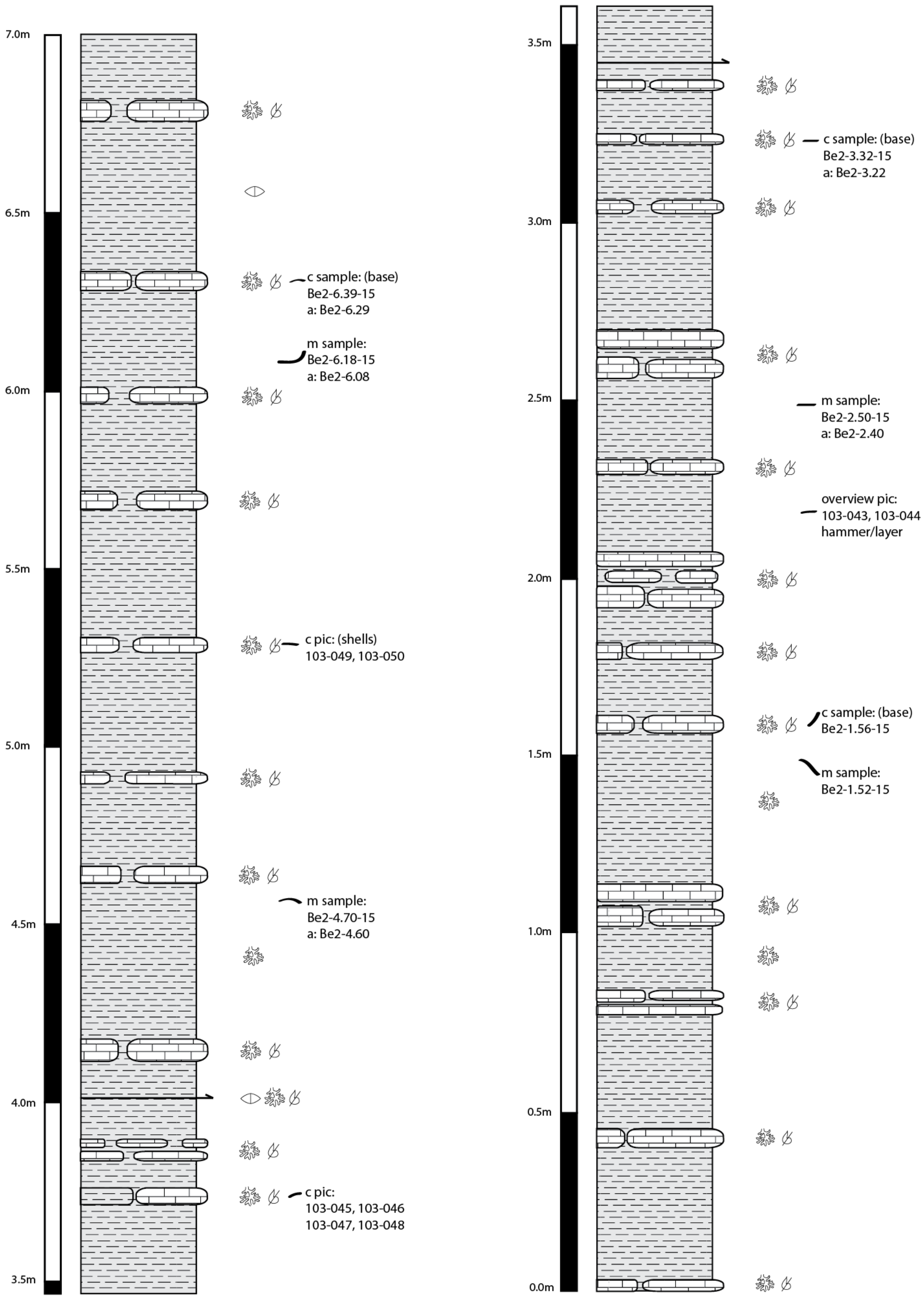

Appendix 2.3: Vollen measured section

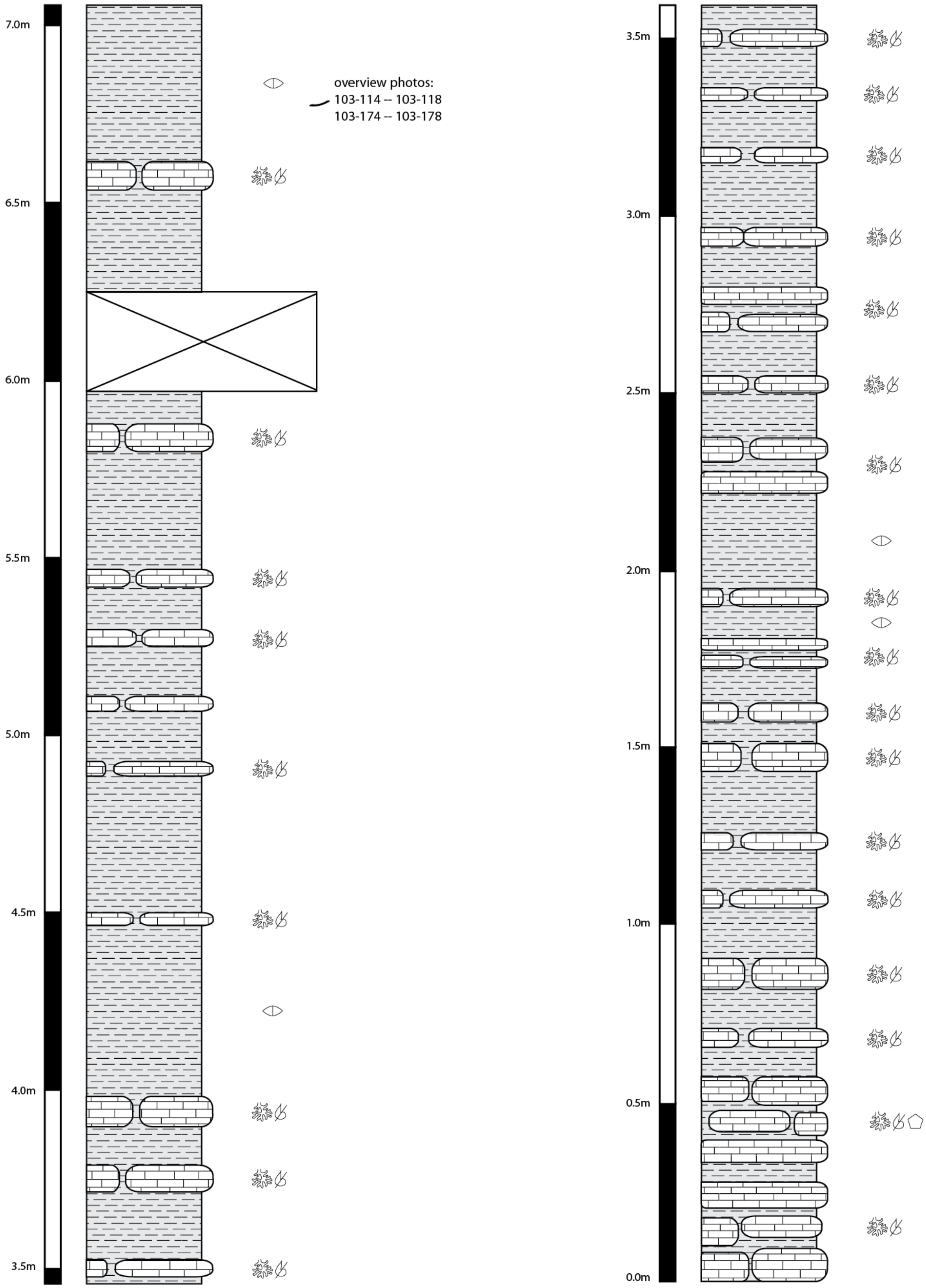

Appendix 2.4: Elnestangen measured section

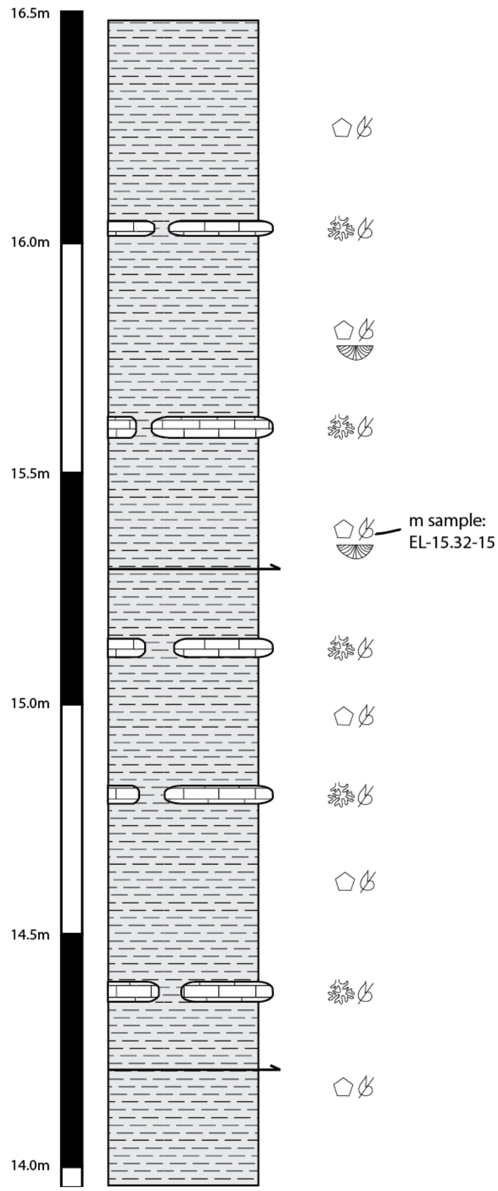

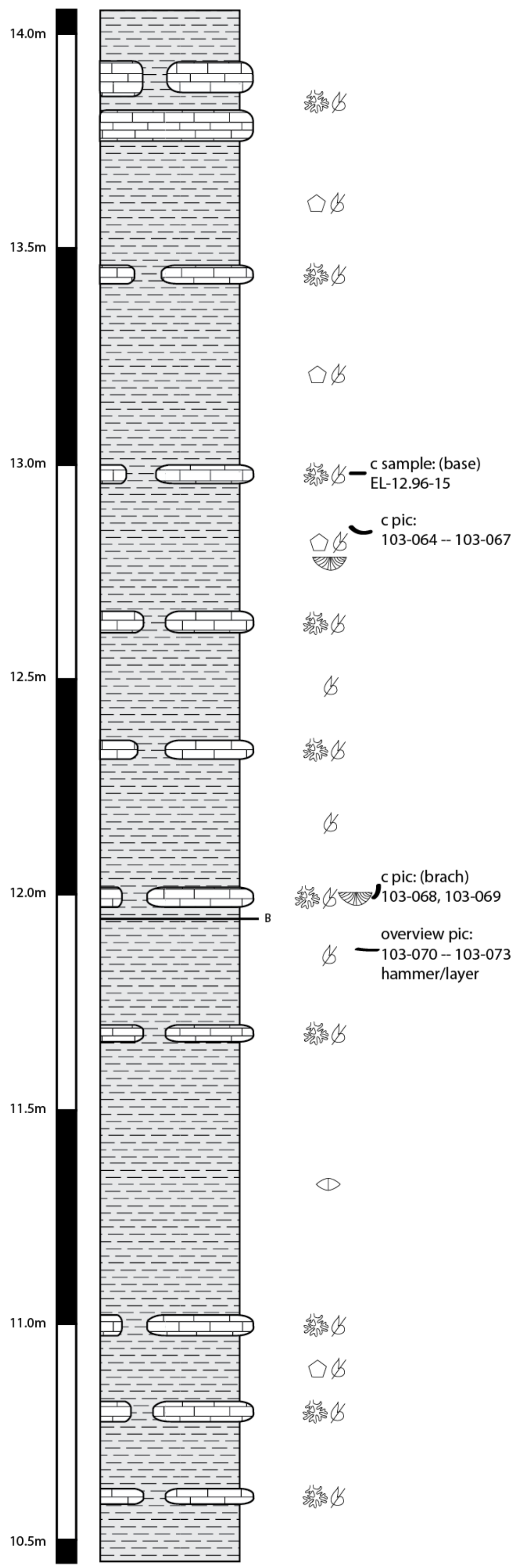
14.0m
13.5m
13.0m
12.5m
12.0m
11.5m
11.0m
10.5m
c sample: (base)
EL-12.96-15
c pic:
103-064 -- 103-067
c pic: (brach)
103-068, 103-069
B
overview pic:
103-070 -- 103-073
hammer/layer

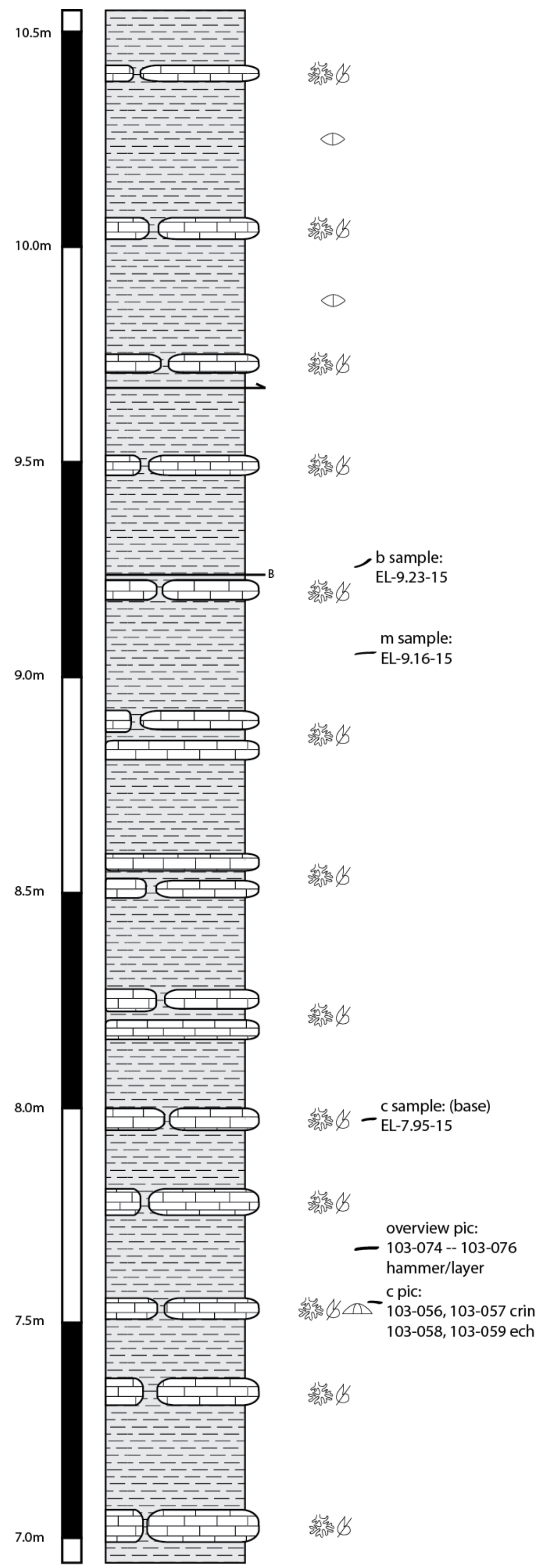
10.5m
10.0m
9.5m
9.0m
8.5m
8.0m
7.5m
7.0m
B
b sample:
EL-9.23-15
m sample:
EL-9.16-15
c sample: (base)
EL-7.95-15
overview pic:
103-074 -- 103-076
hammer/layer
c pic:
103-056, 103-057 crin
103-058, 103-059 ech

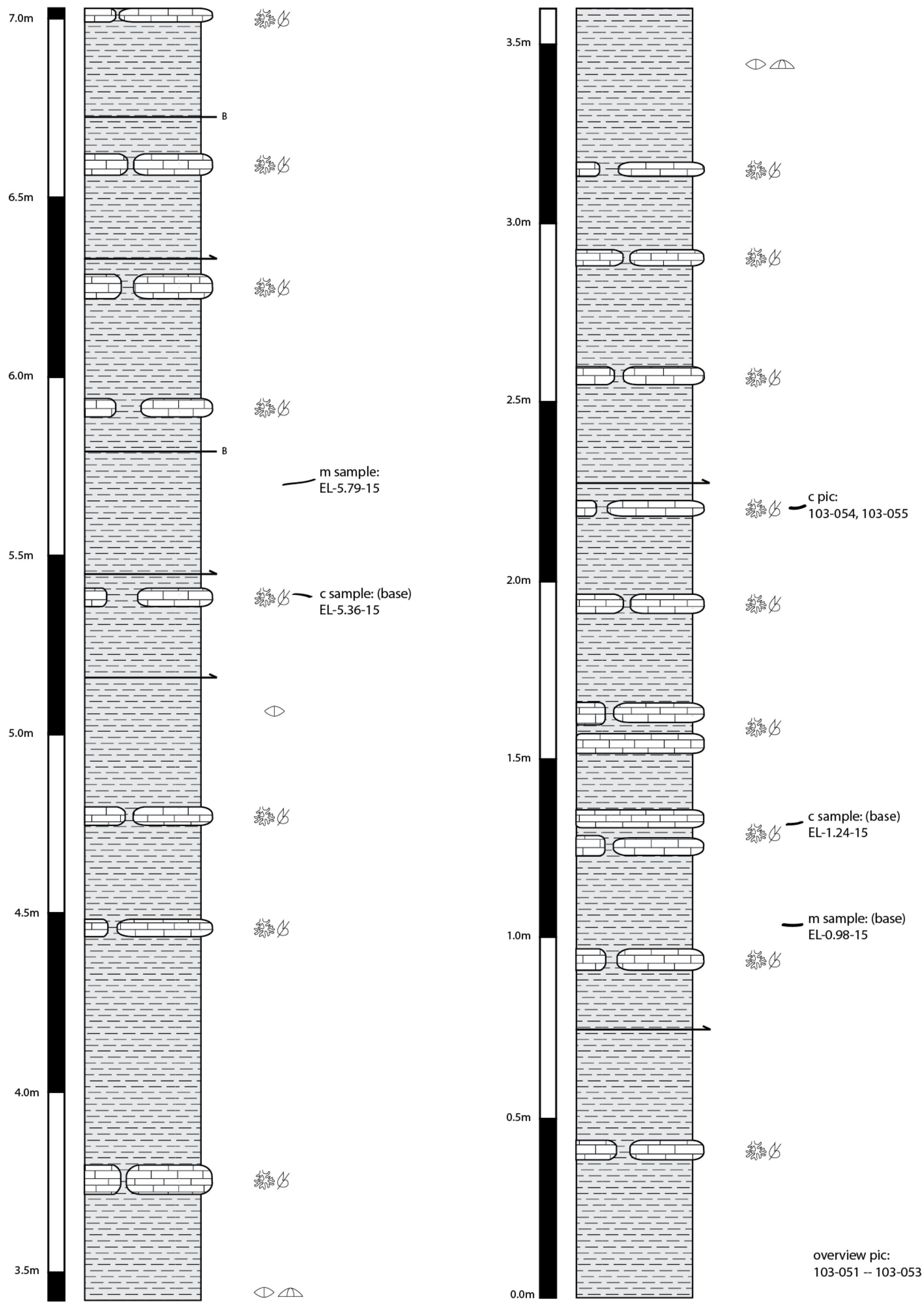
7.0m
6.5m
6.0m
5.5m
5.0m
4.5m
4.0m
3.5m
B
B
m sample:
EL-5.79-15
c sample: (base)
EL-5.36-15
3.5m
3.0m
2.5m
2.0m
1.5m
1.0m
0.5m
0.0m
c pic:
103-054, 103-055
c sample: (base)
EL-1.24-15
m sample: (base)
EL-0.98-15
overview pic:
103-051 -- 103-053

Appendix 2.5: Bentonite Arnestad measured section

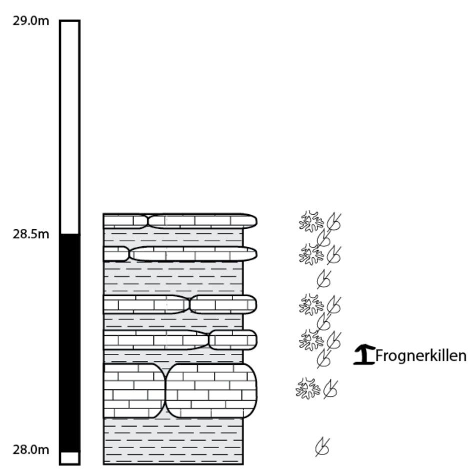


28.0m
27.5m
27.0m
26.5m
26.0m
25.5m
25.0m
24.5m
bentonite
m sample:
BA-25.86-15
a: BA-27.10
overview pic:
103-0159, 103-060
24.5m
24.0m
23.5m
23.0m
22.5m
22.0m
21.5m
21.0m
B
m pic: (bentonite?)
103-0156 -- 103-0158

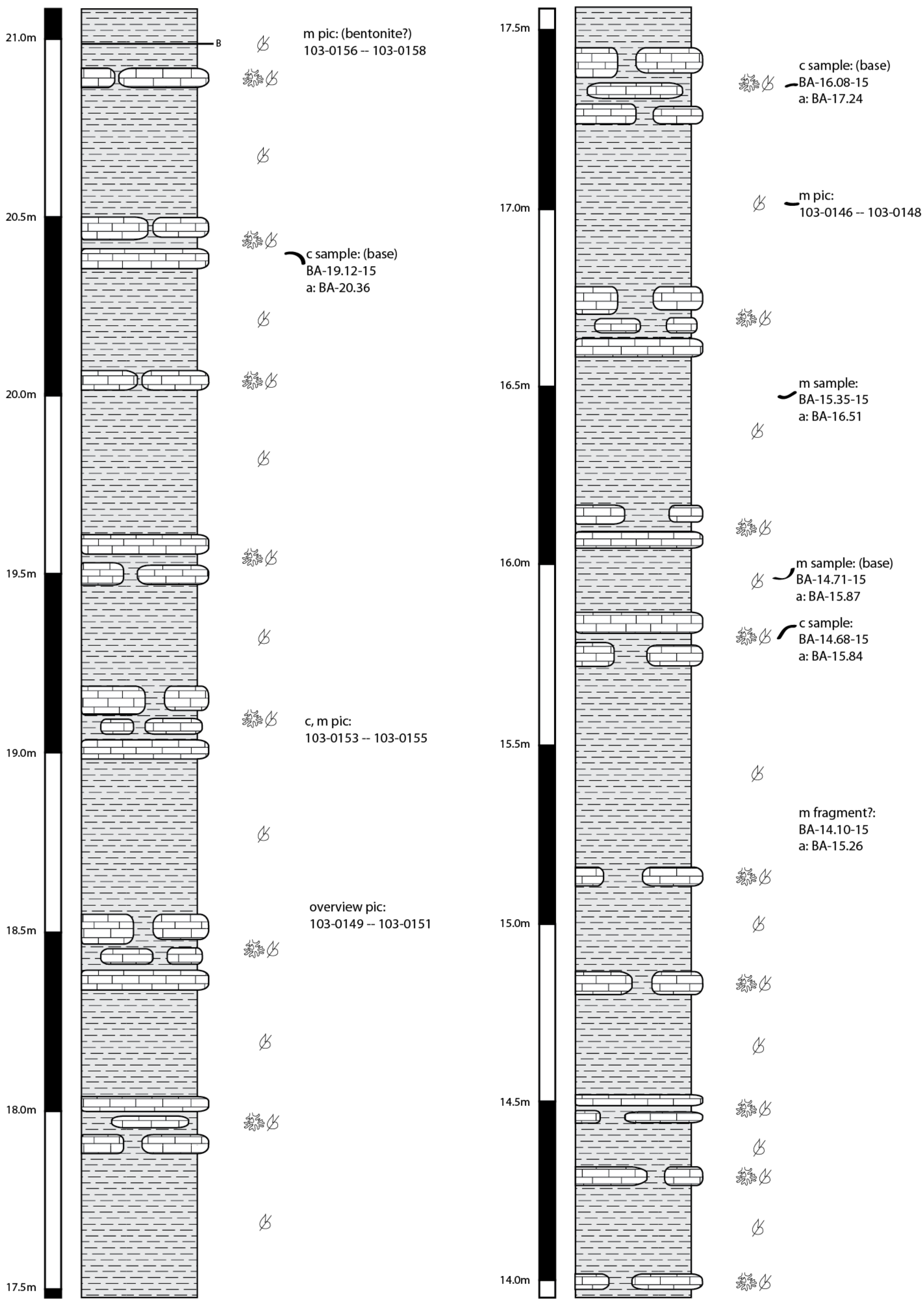

21.0m
20.5m
20.0m
19.5m
19.0m
18.5m
18.0m
17.5m
B
m pic: (bentonite?)
103-0156 -- 103-0158
c sample: (base)
BA-19.12-15
a: BA-20.36
c, m pic:
103-0153 -- 103-0155
overview pic:
103-0149 -- 103-0151
17.5m
17.0m
16.5m
16.0m
15.5m
15.0m
14.5m
14.0m
c sample: (base)
BA-16.08-15
a: BA-17.24
m pic:
103-0146 -- 103-0148
m sample:
BA-15.35-15
a: BA-16.51
m sample: (base)
BA-14.71-15
a: BA-15.87
c sample:
BA-14.68-15
a: BA-15.84
m fragment?:
BA-14.10-15
a: BA-15.26

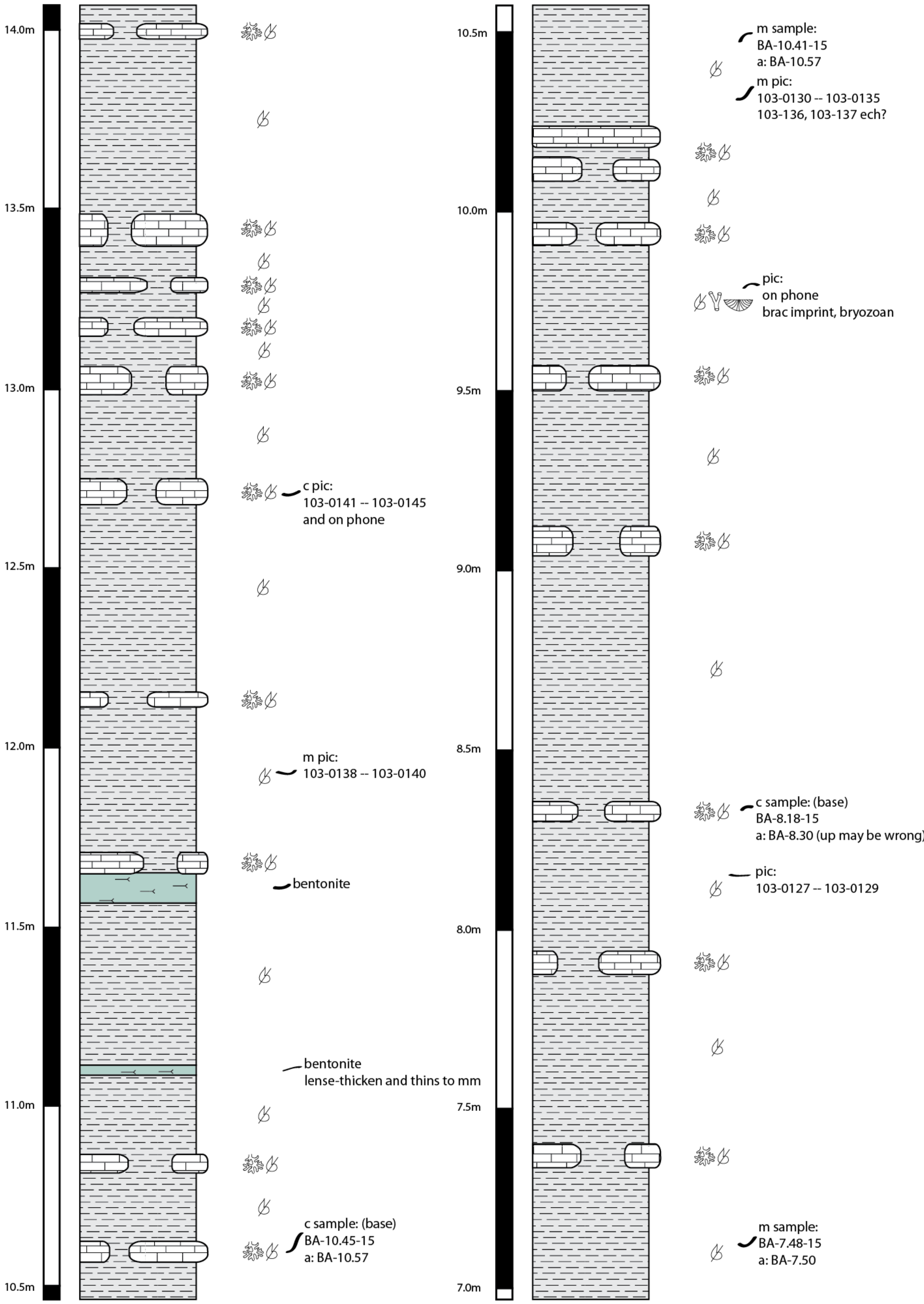
14.0m
13.5m
13.0m
12.5m
12.0m
11.5m
11.0m
10.5m
c pic:
103-0141 -- 103-0145
and on phone
m pic:
103-0138 -- 103-0140
bentonite
bentonite
lense-thicken and thins to mm
c sample: (base)
BA-10.45-15
a: BA-10.57
10.5m
10.0m
9.5m
9.0m
8.5m
8.0m
7.5m
7.0m
m sample:
BA-10.41-15
a: BA-10.57
m pic:
103-0130 -- 103-0135
103-136, 103-137 ech?
pic:
on phone
brac imprint, bryozoan
c sample: (base)
BA-8.18-15
a: BA-8.30 (up may be wrong)
pic:
103-0127 -- 103-0129
m sample:
BA-7.48-15
a: BA-7.50

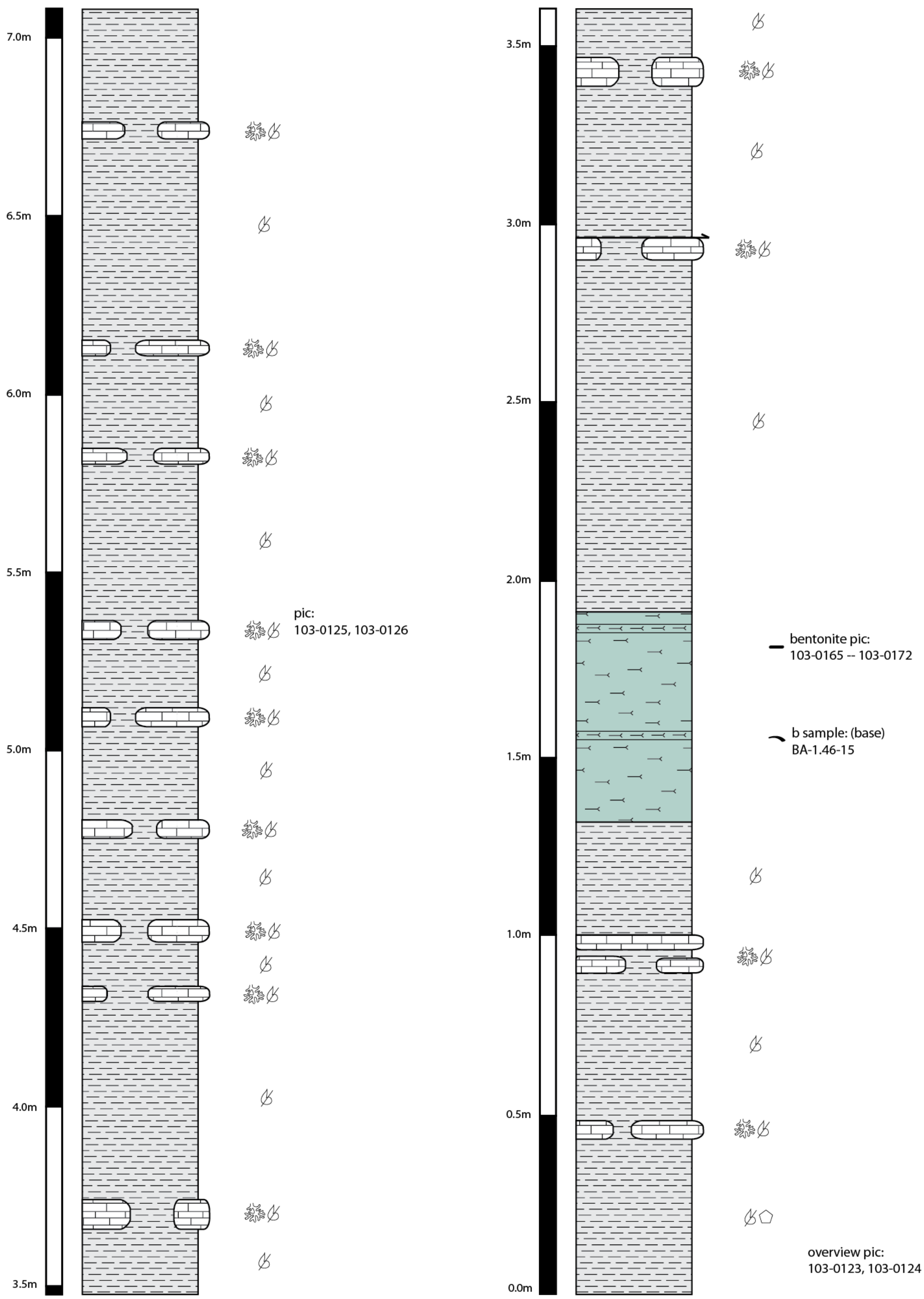
7.0m
6.5m
6.0m
5.5m
5.0m
4.5m
4.0m
3.5m
pic:
103-0125, 103-0126
3.5m
3.0m
2.5m
2.0m
1.5m
1.0m
0.5m
0.0m
bentonite pic:
103-0165 -- 103-0172
b sample: (base)
BA-1.46-15
overview pic:
103-0123, 103-0124

Appendix 2.6: Robben measured section

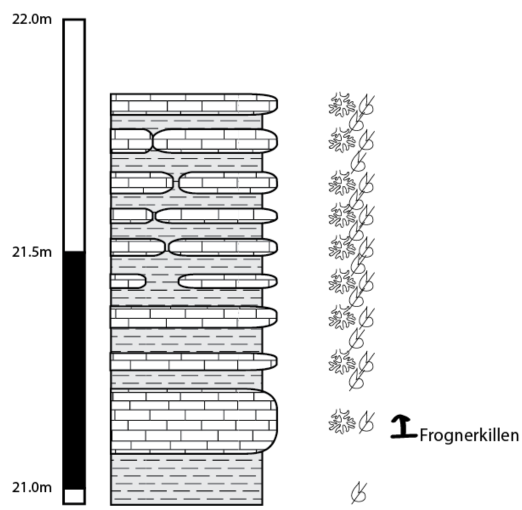

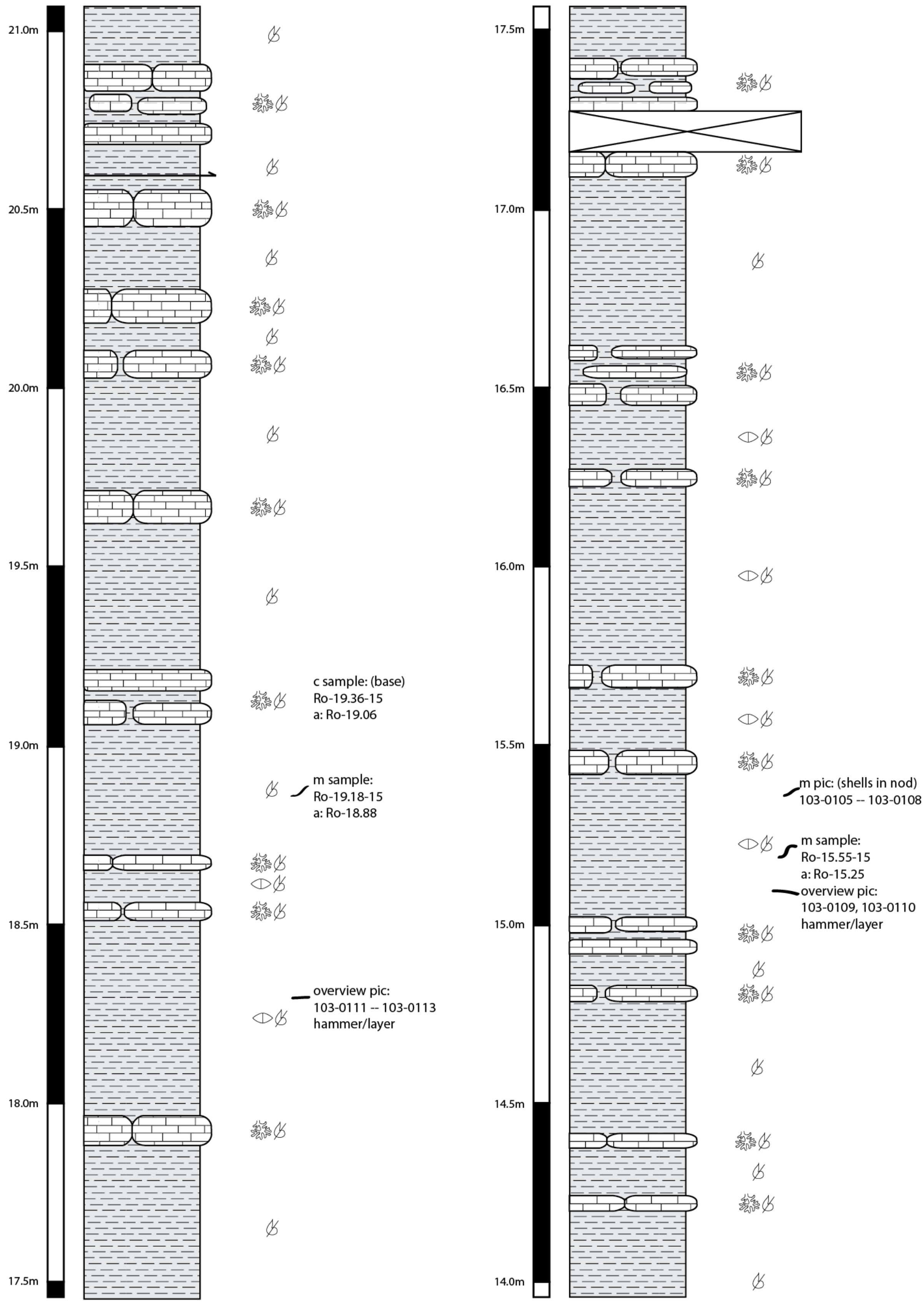
21.0m
20.5m
20.0m
19.5m
19.0m
18.5m
18.0m
17.5m
c sample: (base)
Ro-19.36-15
a: Ro-19.06
m sample:
Ro-19.18-15
a: Ro-18.88
overview pic:
103-0111 -- 103-0113
hammer/layer
17.5m
17.0m
16.5m
16.0m
15.5m
15.0m
14.5m
14.0m
m pic: (shells in nod)
103-0105 -- 103-0108
m sample:
Ro-15.55-15
a: Ro-15.25
overview pic:
103-0109, 103-0110
hammer/layer

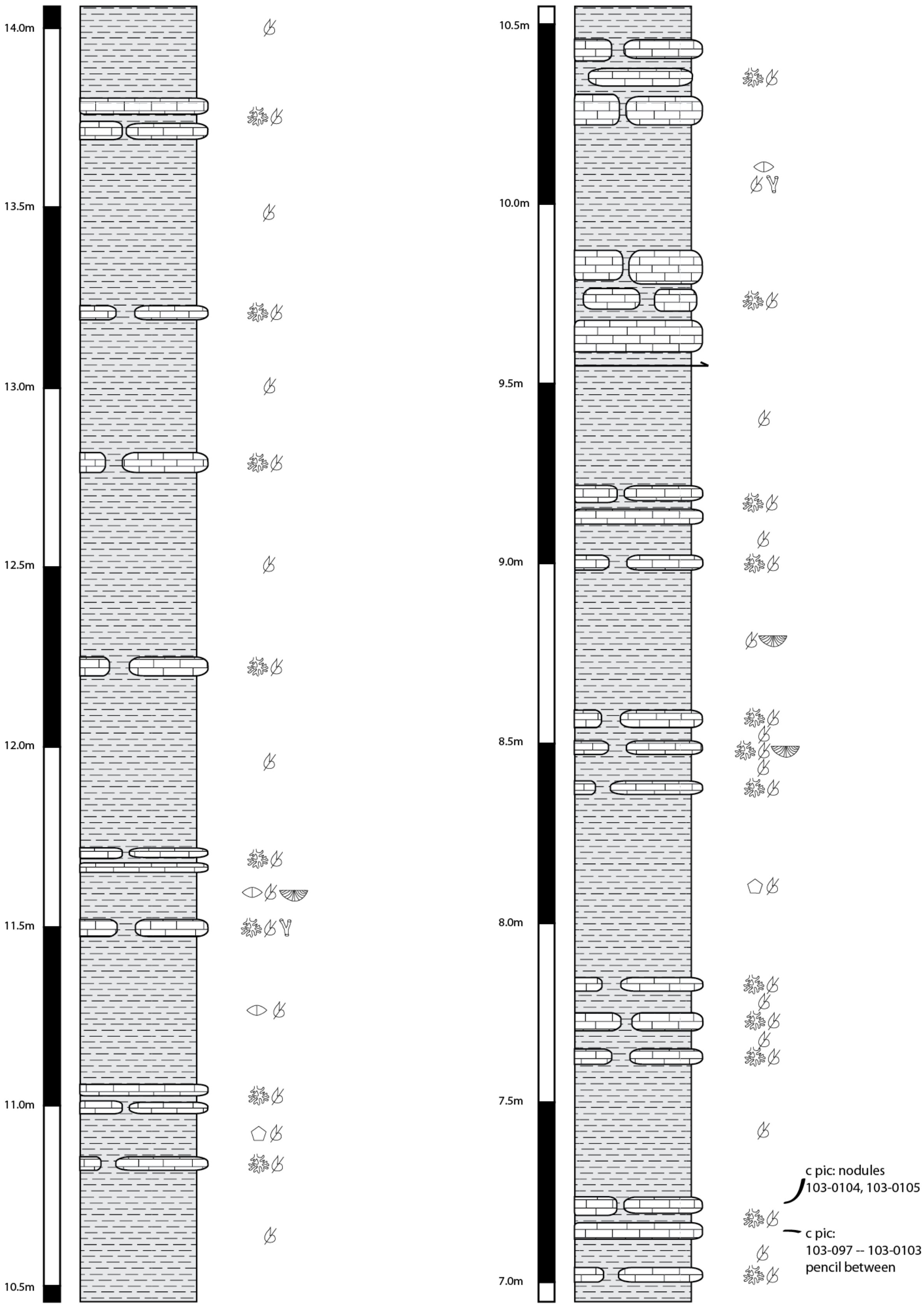
14.0m
13.5m
13.0m
12.5m
12.0m
11.5m
11.0m
10.5m
10.5m
10.0m
9.5m
9.0m
8.5m
8.0m
7.5m
7.0m
c pic: nodules
103-0104, 103-0105
c pic:
103-097 -- 103-0103
pencil between

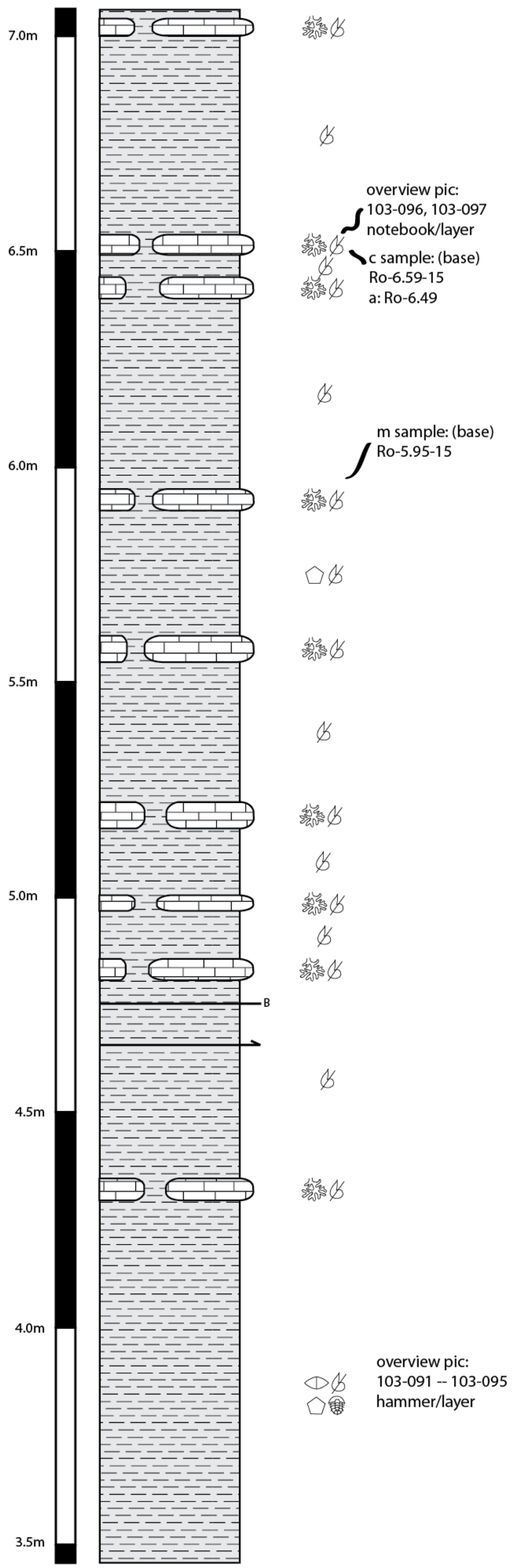

7.0m
6.5m
6.0m
5.5m
5.0m
4.5m
4.0m
3.5m
overview pic:
103-096, 103-097
notebook/layer
c sample: (base)
Ro-6.59-15
a: Ro-6.49
m sample: (base)
Ro-5.95-15
B
overview pic:
103-091 -- 103-095
hammer/layer

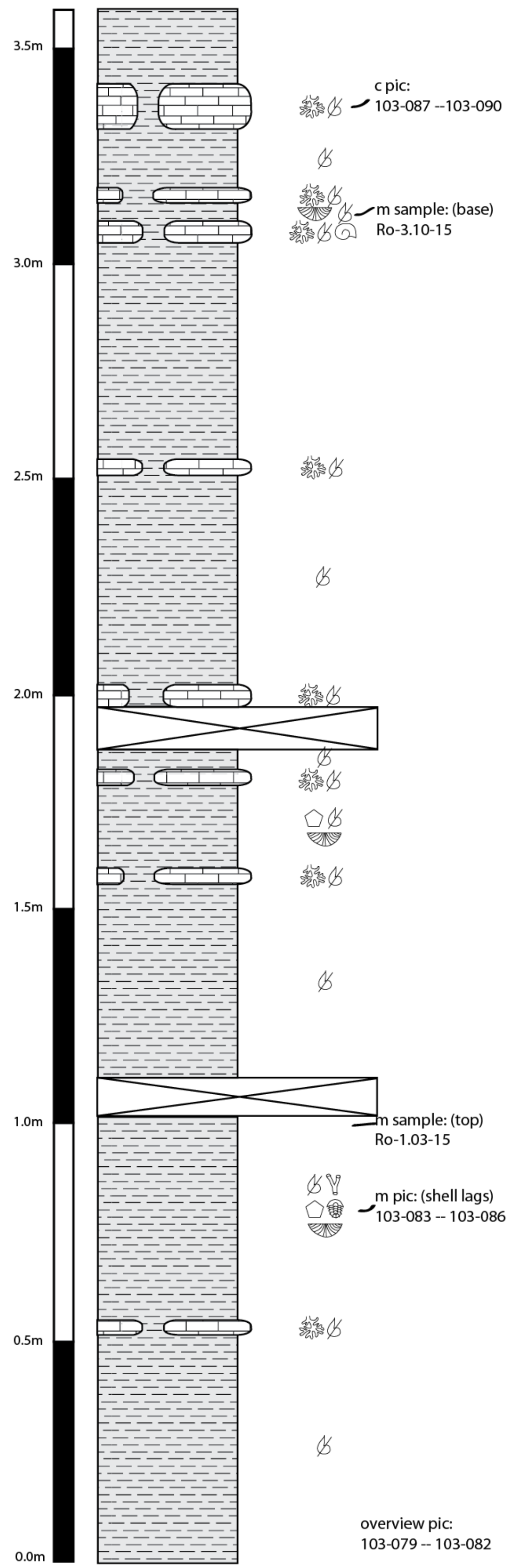

3.5m
3.0m
2.5m
2.0m
1.5m
1.0m
0.5m
0.0m
c pic:
103-087 --103-090
m sample: (base)
Ro-3.10-15
m sample: (top)
Ro-1.03-15
m pic: (shell lags)
103-083 -- 103-086
overview pic:
103-079 -- 103-082